# Cell surface receptor kinase FERONIA linked to nutrient sensor TORC signaling controls root hair growth at low temperature linked to low nitrate in *Arabidopsis thaliana*

Javier Martínez Pacheco[1,*], Limei Song[2,3,*], Lenka Kuběnová[4], Miroslav Ovečka[4], Victoria Berdion Gabarain[1], Juan Manuel Peralta[1], Tomás Urzúa Lehuedé[5,6], Miguel Angel Ibeas[5,6], Martiniano M. Ricardi[7], Sirui Zhu[2], Yanan Shen[2], Mikhail Schepetilnikov[8], Lyubov A Ryabova[8], José M. Alvarez[5,10], Rodrigo A. Gutierrez[9,10], Guido Grossman[11], Jozef Šamaj[3], Feng Yu[2,†] & José M. Estevez[1,5,6,10,†]

[1]Fundación Instituto Leloir and IIBBA-CONICET. Av. Patricias Argentinas 435, Buenos Aires C1405BWE, Argentina.
[2]State Key Laboratory of Chemo/Biosensing and Chemometrics, College of Biology, and Hunan Key Laboratory of Plant Functional Genomics and Developmental Regulation, Hunan University, Changsha 410082, P.R. China.
[3]Laborarory of Species Interaction and Biological Invasion, School of Life Science, Hebei University, Baoding 071002, P.R. China
[4]Department of Biotechnology, Faculty of Science, Palacký University Olomouc, Šlechtitelů 27, 783 71 Olomouc, Czech Republic.
[5]Centro de Biotecnología Vegetal, Facultad de Ciencias de la Vida, Universidad Andres Bello.
[6]ANID - Millennium Nucleus for the Development of Super Adaptable Plants (MN-SAP), Santiago, Chile.
[7]Instituto de Fisiología, Biología Molecular y Neurociencias (IFIBYNE-UBA-CONICET) and Facultad de Ciencias Exactas y Naturales, Universidad de Buenos Aires, Ciudad Universitaria, Buenos Aires, Argentina.
[8]Institut de Biologie Moléculaire des Plantes, CNRS, UPR 2357, Université de Strasbourg, Strasbourg, France.
[9]Centre FONDAP Center for Genome Regulation, Santiago, Chile; Departamento de Genética Molecular y Microbiología, Facultad de Ciencias Biológicas, Pontificia Universidad Católica de Chile, Santiago, Chile.
[10]ANID - Millennium Institute for Integrative Biology (iBio), Santiago, Chile.
[11]Institute of Cell and Interaction Biology, Heinrich-Heine-University Düsseldorf, Germany; Cluster of Excellence in Plant Sciences, Heinrich-Heine-University Düsseldorf, Germany.

*Co-first authors.
[†]Correspondence should be addressed. Email: feng_yu@hnu.edu.cn (F.Y) and jestevez@leloir.org.ar (J.M.E)

**Abstract**

Root hairs (RH) are excellent model systems for studying cell size and polarity since they elongate several hundred-fold their original size. Their tip growth is determined both by intrinsic and environmental signals. Although nutrient availability and temperature are key factors for a sustained plant growth, the molecular mechanisms underlying their sensing and downstream signaling pathways remain unclear. Here, we identified that low temperature (10°C) triggers a strong RH elongation response involving the cell surface receptor kinase FERONIA (FER) and the nutrient sensing TOR Complex 1 (TORC). In this study, we found that FER is required to perceive limited nutrient availability caused by low temperature. FER interacts with and activates TORC-downstream components to trigger RH growth. In addition, the small GTPase Rho-related protein from plants 2 (ROP2) is also involved in this RH growth response linking FER and TOR. We also found that limited nitrogen nutrient availability can mimic the RH growth response at 10°C in a NRT1.1-dependent manner. These results uncover a molecular mechanism by which a central hub composed by FER-ROP2-TORC is involved in the control of RH elongation under low temperature and nitrogen deficiency.

Abstract Word counts 186

Text Word counts 3,885
Figures 1-7

Passwords: Arabidopsis, cell surface, FERONIA, nitrogen, low temperature, root hairs, ROP2, TOR kinase.

65 **Introduction**

66

67 Root hairs (RH) are cell outgrowths that develop as cylindrical protrusions from the root
68 epidermis in a developmentally regulated manner[1]. RHs are able to expand in a polar manner
69 several hundred times their original size in a couple of hours to reach water-soluble nutrients in
70 the soil, to promote interactions with the local microbiome, and to support the anchoring of the
71 plant[2]. RH growth is controlled by the coordination of a plethora of environmental and
72 endogenous factors[3,4]. Recently, an autocrine mechanism of RH growth was described where
73 RALF1-FER complex recruits and phosphorylates the early translation initiation factor 4E1
74 (eIF4E1) to enhance protein synthesis of specific mRNAs, including the RH growth master
75 regulator *ROOT HAIR DEFECTIVE SIX-LIKE4 (RSL4)*[5]. The observation that RH cells can respond to
76 their local environment in a cell-autonomous manner within minutes[6], points towards
77 mechanisms that directly modulate the growth machinery at the growing apex.

78

79 It is known that macronutrient availability is a key factor that promotes rapid RH growth[3,7,8]
80 Recently, we showed that under low temperature conditions (10°C), nutrient availability in the
81 media is reduced and triggers an enhanced RH growth that is suppressed if nutrients are
82 increased[9]. We specifically showed that RH growth of WT Col-0 plants is highly responsive to
83 increasing nutrient concentrations (from 0.5X Murashige and Skoog (MS) to 2.0X MS) with regular
84 concentration gelling agents (0.8%). High nutrient concentration impairs RH growth even if they
85 are exposed to low temperatures. In a similar manner, an increase in agar concentration (from
86 0.8% to 2.5%) in the MS medium, which likely restrains nutrient mobility and nutrient uptake[10–13]
87 blocked low temperature-induced RH elongation[9]. These observations suggested that low
88 temperature restrict nutrient mobility and availability in the culture medium, leading to
89 promotion of polar RH growth. It is still unclear which specific nutrients are affected and the
90 signaling pathways involved in the temperature effect that triggers this RH growth response.
91 Diminished nutrient availability is known to activate RH expansion through a transcriptional
92 reprogramming governed by the transcription factors (TF) RHD6-RSL4[9]. Specifically, a novel
93 ribonucleoprotein complex composed of lncRNA AUXIN-REGULATED PROMOTER LOOP (APOLO)
94 and the TF WRKY42 forms a regulatory hub to activate RHD6 by shaping its epigenetic
95 environment and integrate low temperature signals governing RH growth[9,14]. In addition, we
96 recently identified new molecular components involved in low temperature RH growth. We
97 found that cell wall-apoplastic related peroxidases, PRX62 and PRX69, are important for low
98 temperature triggered RH growth by inducing changes in ROS homeostasis and cell wall EXTENSIN
99 insolubilization[15]. Although relevant advances have been achieved in our understanding on how
100 RH growth occurs at low temperature, it is still unclear how nutrient availability caused by low
101 temperature is perceived in the RH cells and the extent of molecular responses that control RH
102 growth.

103

104 TARGET OF RAPAMYCIN (TOR) is an evolutionarily conserved Ser/Thr protein kinase in all
105 eukaryotic organisms that acts as a central growth regulator controlling metabolism and protein
106 synthesis[16–18]. TOR is found in at least two distinct multiprotein complexes called TOR Complex 1
107 and 2 (TORC1 and TORC2) in animal cells, although only the equivalent for TORC1 has been
108 experimentally validated in plants[19,20]. The *Arabidopsis* TOR complex is encoded by one *TOR* gene
109 (*At*TOR)[21], two *REGULATORY-ASSOCIATED PROTEIN OF TOR (RAPTOR 1A and 1B)* genes[22–27], and
110 two *LETHAL WITH SEC THIRTEEN 8 (LST8)* genes[28]. In contrast to the embryo-lethal *tor*-null
111 mutant lines, *raptor1b* and *lst8-1* mutants are viable but show significant growth defects and
112 developmental phenotypes[29]. Some canonical downstream targets of TOR are conserved in
113 plants, such as the 40S ribosomal S6 kinase (S6K) which stimulates protein synthesis[24,30–33]. In
114 plants, TOR complex plays a key role during many stages of the plant life cycle by controlling both
115 anabolic and catabolic downstream processes. In addition, TOR is activated by nutrient
116 availability and inactivated by stresses that alter cellular homeostasis[18,34–38]. The TOR complex
117 senses and integrates signals from the environment to coordinate developmental and metabolic
118 processes including hormones (e.g., auxin), several nutrients (e.g., nitrogen and sulfur), amino
119 acids and glucose[16,27,39–43]. However, the underlying molecular mechanism by which TOR
120 operates at a single plant cell level has yet to be elucidated.

121

122 To date, few upstream regulators of TOR have been described in plants. Among them, there is a
123 subfamily of small GTPase Rho-related protein from plants (ROPs) involved in the spatial control
124 of cellular processes by signaling to the cytoskeleton and vesicular trafficking. Particularly, ROP2
125 activates TOR in response to auxin and nitrogen signals[43–45]. ROP2 is described as a monomeric
126 GTP-binding protein that participates in many cellular signaling processes, including the polar
127 growth of pollen tubes and root hairs[46–49]. ROP activation is regulated by ROP guanine nucleotide
128 exchange factors (ROP-GEFs) which interact with several receptor-like kinases (RLKs) including
129 the *Cr*RLK family member FERONIA (FER)[47]. During the elongation of RH, ROP2 is activated by the
130 ROPGEF1-FER interaction. This process is also regulated by ROP-GEF4 and ROP-GEF10[47,50]. FER
131 was also linked to carbon/nitrogen balance during plant growth[51]. Even more, it was shown that
132 the cytoplasmic kinase domain of FER and its partner RIPK (RPM1-induced protein kinase)
133 interact with TOR and RAPTOR-1B forming a complex to positively modulate the TOR pathway
134 under low nitrogen nutrient conditions[52]. Currently, it is clear that plant growth can be regulated
135 via the FER-TOR pathway as it links amino acid and/or nutrients signaling with true leaves
136 development[51]. This evidence suggests that nutrient-mediated sensing at the cell surface level
137 triggers a response using the TOR signaling pathway. However, it is still unknown which are the
138 environmental signals activated in RH by the FER-TOR pathway in RH. Considering that low
139 temperature stress can result in enhanced RH growth[9,14], this stress condition was used as a
140 proxy to investigate environmental signals that activate RH cell elongation. Our research reveals a

141 novel mechanism in which FER, ROP2 and TOR are necessary to regulate RH growth in
142 *Arabidopsis* in the context of the nitrogen nutrient availability as caused by low temperature
143 stress.
144
145 **Results**
146
147 **FER is required to trigger a strong RH growth response at low temperature.** We asked which
148 might be the RH surface protein involved in perceiving or transducing the low temperature
149 stimulus. Since CrRLK1L FER was shown as an important hub between the cell surface signaling
150 and downstream processes during RH growth[5,47], we tested whether *fer-4* null mutant or *fer-5* (a
151 truncated version with shortened kinase domain (KD)) can respond to low temperature stimulus
152 (**Figure S1A**). Both *fer* mutants failed to trigger RH growth at low temperature (**Figure 1A**). We
153 considered plant genotype (Geno), treatment (Temp), and the interaction between genotype and
154 treatment (Geno:Temp) as the factors for two-way analysis of variance (ANOVA) to define
155 significant changes in RH growth in response to cold. We determined that the genotype factor
156 has a substantial and significant effect on RH growth in *fer-4* and *fer-5* mutants. Notably, the
157 Geno:Temp interaction term is also significant for *fer-4* and *fer-5*. These results suggest that FER
158 contributes to general RH growth and RH response to cold (**Figure S1B**). In contrast, the mutant
159 *eru*, impaired in the related CrRLK1L ERULUS (ERU), previously linked to RH growth and cell wall
160 integrity processes with very short RH phenotype at 22°C[53,54], was able to react to low
161 temperature which triggered RH growth response although to a lower extent than wild-type Col-0
162 plants (**Figure 1A**). This indicates that FER, but not ERU, might be involved specifically in this
163 growth response despite being phylogenetically related[54]. Then, a fluorescent translational
164 reporter line of FER (*p*FER:FER-GFP), was used to study *FER* expression in roots and RH. FER
165 protein levels are increased clearly activated in root cells under low temperature stimulus (**Figure**
166 **1B**), and during RH growth (**Figure 1C**). Distribution of FER-GFP in the clear zone and punctate
167 compartments in the cytoplasm was not affected by the temperature change from 22°C to 10°C.
168 However, accumulation of FER-GFP at the plasma membrane was increased at low temperature
169 (at 10°C) (**Figure 1C**). Finally, phosphorylated, and non-phosphorylated levels of FER (FER-p/FER)
170 were quantified at both temperatures. Under low temperature, almost half of the FER protein
171 levels were present as a non-phosphorylated form and after 3 days of growth, almost all FER
172 protein was present as a phosphorylated version (**Figure 1D**). This indicates that low temperature
173 not only increases FER protein levels at the plasma membrane of growing RH, but also promotes
174 a complete phosphorylation of FER protein. This is possibly enhancing the interaction with
175 putative partners and triggering the activation of downstream signaling components of RH polar
176 growth.
177

178 **TOR pathway is involved in low temperature induced RH growth.** Recently, it was shown that
179 FER-RIPK interacts with TOR-RAPTOR1B and phosphorylates it leading to TOR pathway activation
180 in the context of nutrient perception and regulation of global metabolism[52]. We then asked
181 whether TOR might be also involved in the RH growth process under low temperature. We used a
182 β-estradiol (es)-induced TOR knockdown (*tor-es,* es-induced RNAi silencing of TOR) line[55] which
183 showed short RH as reported previously[32]. Notably, induction of TOR silencing with estradiol
184 completely blocked the RH response to low temperature (**Figure 2A**). Similarly, inhibition of TOR
185 kinase activity with AZD-8055[56], an ATP-competitive inhibitor of mTOR kinase activity, abolished
186 the RH growth at both 22°C and low temperature (**Figure 2B**). Overexpression of TOR enhanced
187 RH growth at both temperatures assayed (**Figure 2C**). Using two-way ANOVA analysis, we found
188 that alteration of TOR levels impacts general RH growth (Geno factor, **Figure S2A**). However, the
189 significant interaction between genotype and treatment indicates TOR is also involved in RH
190 responses to cold (Geno:Temp, **Figure S2A**). These results suggest that the TOR pathway is
191 involved in the RH growth and specifically in RH low temperature growth response and might
192 operate downstream of FER. At the transcriptional level, TOR root expression level is upregulated
193 up to three-folds at 10°C vs 22°C (**Figure S2B**). We tested whether the growth response at low
194 temperature in RH is also affected in mutants of the TOR pathway and some downstream
195 components. All the plant mutants tested *(raptor1b, rps6b,* and *lst8-1)* were unable to respond to
196 the low temperature treatment. They exhibited a broad spectrum of RH phenotypes as compared
197 to Wt Col-0 plants (**Figure 2C**). For instance, *raptor1b* behaved similarly to *tor-es* mutant, while
198 *rps6b* showed an intermediate phenotype and *lst8* was comparable to Wt Col-0 plants (at 22°C)
199 (**Figure 2C**). In addition, overexpression of TOR and the S6 KINASE 1 (S6K1), a direct downstream
200 target of TOR, showed enhanced RH growth at 22°C. Since previous reports showed
201 phosphorylation of the S6K1 can be used to monitor TOR protein kinase activity in plants[32,55], we
202 measured ratios of S6K-p/S6K. Strong induction of the S6K-p/S6K ratio was observed in Wt Col-0
203 under low temperature (**Figure 2D**). These results suggest TOR and some downstream
204 components (e.g. S6K and RPS6b) are required to promote RH growth under low temperature.
205
206 **FER facilitates TOR polar localization in RH and activation of TOR pathway at low temperature.**
207 Since TOR activation under a plethora of stimuli usually triggers phosphorylation of the
208 downstream factor S6K (S6K-p), we asked whether low temperature responses regulated by FER
209 might control this output. We investigated the molecular mechanisms by which TOR-S6K are
210 induced at 10°C and we tested whether this might be mediated by FER. Since *fer-4* and *tor-es*
211 showed similar RH phenotypes at low temperature (**Figure 2A-B**), possibly indicating that they
212 may act in the same pathway, we first tested whether FER and TOR interaction is enhanced under
213 10°C vs 22°C. By performing a co-immunoprecipitation (Co-IP) analysis, we found that FER-TOR
214 interaction is enhanced under low temperature (**Figure 3A**). This result suggests an interaction
215 between FER and TOR kinase is implicated in RH growth under low temperature. This

216 corroborates previous findings that showed direct interaction of the FER kinase domain and the
217 N-terminal domain of TOR (aa 1-1449 of TOR, NTOR)[52]. Next, we evaluated TOR levels in growing
218 RH by immunolocalization. We found that FER is required for the apical accumulation of TOR
219 since TOR lost the polar pattern in *fer-4* root hairs. However, the level of RH tip-localized TOR
220 detected was similar at both, low temperature, and control conditions (22°C) (**Figure 3B-C** and
221 **Figure S3**). This result indicates that localization of TOR at RH tip is dependent on FER. Then, we
222 tested whether FER is involved in S6K activation by TOR. We measured S6K-p/S6K protein ratio
223 under both growth conditions in Wt Col-0, *fer-4*, *fer-5*, and FER$^{K565R}$ (which has been shown to
224 abolish FER autophosphorylation and transphosphorylation in an *in vitro* kinase activity assay[57,58],
225 although some activity might remain[59]). Interestingly, low temperature enhanced S6K-p levels
226 after 3 days of growth in Wt Col-0 this was partially suppressed in all three *fer* mutants tested
227 (**Figure 3D**). This suggests that FER controls the level of TOR activation under low temperature in
228 RH. Collectively, these results indicate that TOR localization in the RH tip and TOR activation is
229 dependent on FER and enhanced at low temperature.
230
231 **ROP2 is required for low temperature RH growth.** Previous studies have shown a key role of
232 ROP2 in the regulation of RH polarity and elongation[48,60,61], as an important molecular link
233 between FER and downstream components involved in RH growth[47]. In addition, ROP2 promotes
234 the activation of TOR and its relocation to the cell periphery and induces the downstream signal
235 transduction pathway[44]. More importantly, ROP2 was shown to integrate diverse nitrogen and
236 hormone signals for TOR activation[43]. We asked whether low temperature (10°C) is able to
237 change ROP2 targeting (as ROP2p:ROP2-mCitrine) to the plasma membrane in roots and RH. Low
238 temperature (10°C) led to noticeable increase of ROP2 fluorescence intensity in root cells (**Figure**
239 **4A**), in the apical and subapical cytoplasm, and at the apical plasma membrane of RH (**Figure 4B**).
240 Then, we observed that *rop2* and *rop2 rop4* partially abolishes the differential growth responses
241 at 10°C and produces a very short RH phenotype (**Figure 4C**). On the contrary, ROP2 OE triggers a
242 constitutive RH growth at both temperatures (**Figure S4**) similarly to *S6K1 OE* and *TOR OE* lines
243 (**Figure 2C**). In addition, when ROP2 OE is expressed in the *fer* mutant background *fer-8* (ROP2
244 OE/*fer-8*; **Figure S4**), this strong growth effect disappears highlighting the role of FER on the ROP2
245 function. On the other hand, while high levels of TOR enhance RH growth regardless of the
246 temperature treatments, the constitutively active ROP2 version (CA-ROP2) is able to abolish TOR
247 activation of RH growth (**Figure 4C**). The levels of S6K-p/S6K in TOR OE, with constitutive long RH
248 at both temperatures, was reduced by the presence of CA-ROP2 (in TOR OE/CA-ROP2), which
249 correlates with a diminished RH growth (**Figure 4D**). Taken together, we suggest a direct function
250 of ROP2 (and possibly ROP4) at the RH tip. ROP2 function is dependent on the presence of FER
251 and it modulates TOR activity in the RH growth responses to low temperature.
252

253 **Nitrate perception and transport mediated by NRT1.1 controls RH growth at low temperature.**
254 Nitrate is a key nitrogen nutrient required for plant growth and development[62–64]. The
255 CHLORINA1/NITRATE TRANSPORTER1.1 (CHL1/NRT1.1) is the only known nitrate receptor
256 (transporter and receptor) [65–67] as well as for auxin transport[68]. NRT1.1 belong to the low affinity
257 nitrate transporter family. However, when NRT1.1 is phosphorylated at threonine 101, it behaves
258 as a high-affinity $NO_3^-$ (nitrate) transporter, giving this protein a dual-affinity capability[69–72].
259 Previous studies have shown that nitrogen and specifically nitrate is important for TOR
260 signaling[43,73]. Since low temperature growth conditions reduce nutrient availability in the media
261 and trigger a strong response in RH growth[9,14], we hypothesized that the nitrate signaling
262 pathway was involved. We directly test this hypothesis, and we measured using a qualitative
263 method the temperature effect of $NO_3^-$ diffusion in agar plates at 22°C and at 10°C (**Figure S5**). As
264 expected, the $NO_3^-$ diffusion at 22°C was twice as high as at 10°C, confirming our previous results
265 that the temperature effect affects the amount of nitrates available for the roots and RHs[9,14]. In
266 agreement, we found that high levels of nitrate (18.8 and 37.6 mM) supplied in the M407 media
267 without nitrogen (see methods) were able to partially repress low temperature-mediated RH
268 growth while low levels of nitrate (0.5 mM) did not affect growth under this temperature (**Figure**
269 **5A**). As a reference, previous experiments were carried out with 0.5X MS media containing 9.3
270 mM of nitrate and several other compounds (see **Table S1**). In addition, an increase in agar
271 concentration in the 407 media (from 0.8% to 1.5%) even with high $NO_3^-$ (18.8 mM), which likely
272 restrains $NO_3^-$ diffusion mobility induced RH expansion independently of the temperature (**Figure**
273 **S5**). Three-way ANOVA analysis across all conditions (**Figure S6A and S6B**) reveals that
274 temperature (T), the interaction of agar with $NO_3^-$ (agar:N); and the interaction of agar,
275 temperature, and $NO_3^-$ (agar:T:N) largely explain the variance of RH elongation; while $NO_3^-$ and
276 agar factors on their own are less influential (**Figure S5C**). Altogether, these observations suggest
277 that low temperatures restrict $NO_3^-$ diffusion and availability in the culture medium, leading to
278 the promotion of polar RH growth. This result indicated nitrate can impact RH cell elongation at
279 low temperature, particularly under low nutrient mobility environment. Next, we tested whether
280 NRT1.1 was involved in this low temperature RH growth response. The NRT1.1 null mutants *chl1-*
281 *5*, *chl1.9* (NRT1.1 harbors a substitution P492L that suppresses its root nitrate uptake activity[8]), as
282 well as the *CHL1*$^{T101D}$ (which mimics phosphorylated version of NRT1.1) showed strong RH growth
283 response regardless of temperature conditions (**Figure 5B**), similarly to *S6K1 OE* and *TOR OE* lines
284 (**Figure 2C**), but to a lower extent in terms of RH elongation. Only the *CHL1*$^{T101A}$
285 (dephosphorylated version of NRT1.1) was able to slightly respond to the change in temperature.
286 As expected, similar levels of S6K-p/S6K were detected in the *chl1-9* line at both temperatures
287 (**Figure 5C**). When these NRT1.1 mutants were grown under high (18.8 mM) or low (0.5mM)
288 nitrate concentrations (high N/low N) at both temperatures (at 22°C and at 10°C), a similar RH
289 phenotype was detected between both nitrate conditions either at 22°C or 10°C (**Figure 5D**). In
290 contrast, Wt Col-0 RH was sensitive to both low temperature and nitrate levels. Taken together,

291 these results suggest low temperature may restrict nitrate accessibility to the RH linked to a
292 lower mobility in the media affecting NRT1.1-mediated signaling upstream of TOR-S6K activation.
293
294
295 **FER-ROP2-TOR hub is required for nitrate starvation-mediated RH growth response**. Recently it
296 was reported that RALF1-FERONIA complex is able to interact with TOR kinase under low N
297 conditions modulating the TOR downstream signaling pathway[52]. As described above, we found
298 that Col-0 grown at 22°C under high N condition have a shorter RH phenotype as compared to
299 low N condition. This growth response is consistent with previous studies in which the RH length
300 in *Arabidopsis* and other species decrease as the nitrate concentration increases although the
301 molecular mechanism remained unknown[60,74]. To gain a better insight into the role of FER and
302 TOR in this process, we decided to test the *fer* mutants, the TOR pathway mutants and selected
303 overexpressing lines (TOR and S6K) in low (0.5 mM) and high nitrate (18.8 mM) media conditions
304 (**Figure 6A** and **Figure S7**). Under low nitrate conditions, the RH response was suppressed in both
305 *fer* mutants and in the *tor-es* inducible mutant compared to Col-0. This result supports the idea
306 that FER and TOR are necessary for the RH growth mediated by low nitrate conditions. The *TOR*
307 *OE* line showed a RH growth phenotype similar to Col-0 under low N and a higher RH growth in
308 excess of N. It is well known that nitrogen starvation causes enhanced root and RH growth,
309 whereas an excess of nitrate inhibits primary root growth[75], because of osmotic stress[71,].
310 Furthermore, plants overexpressing TOR in a nitrate excess medium have a longer primary root
311 phenotype[71]. According to our data that *TOR OE* line showed longer RH than Col-0 under normal
312 conditions (**Figure 6A)**. The constitutive overexpression of TOR can lead not only to a longer
313 primary root but also to longer RH when plants are grown on a high nitrate media to alleviate the
314 nutrient stress. The constitutive active mutant of ROP2 suppressed the TOR OE RH phenotype
315 while *rop2* mutant was unable to respond to contrasting levels of nitrates. A model was proposed
316 where ROP GTPases and the cytoplasmic and apoplastic pH fluctuations can regulate RH tip
317 growth in a nitrogen supply dependent manner thus maintaining the unidirectional growth during
318 the RH elongation[77]. Additionally, nitrate and ammonium levels restore TOR activation under
319 nitrogen-starvation condition via ROP2 activation[43]. We then tested if other components on the
320 TOR complex are also involved in the low nitrate perception linked to RH growth (**Figure 6B).**
321 Similarly to their low temperature phenotype, *raptor1b* and *lst8-1* do not respond with
322 differential RH growth under low nitrate. Mutation of RAPTOR1B resulted in a strong reduction of
323 TOR kinase activity, leading to massive changes in carbon and nitrogen metabolism[78]. The RH
324 phenotype derived from the overexpression of S6K resembled that of TOR OE line (**Figure 6A, 6B**).
325 Altogether, our results show that low-nitrate (low N) RH responses are similar to those
326 determined for low temperature. This is consistent with the idea that nitrate is one of the main
327 signals that trigger RH expansion upon perception by NRT1.1, and subsequently transduction by
328 FER, ROP2 and TOR pathway. We then tested how changed are the levels of S6K-p/S6K as a

329 readout of TOR activation in low N and high N conditions in FER, TOR silenced line (*tor-es*) and
330 NRT1.1 mutants compared to Wt Col-0 (**Figure 6C**). First, Wt Col-0 showed an increased in S6K-
331 p/S6K ratio in low nitrogen similarly to the low temperature effect. On the contrary, and as
332 expected, *fer-4*, *fer-5* and *tor-es* showed much reduced levels of S6K-p/S6K in both nitrate
333 conditions but much lower in low nitrogen. Importantly, the effect of low N on increasing S6K-p
334 levels is abolished in NRT1.1 mutants (*chl1-9*, *chl1-5* and CHLT101D), which is similar to the
335 results observed under low temperature conditions. These results indicate that nitrate effect on
336 S6K-p/S6K ratio depends on NRT1.1 and the FER-TOR complex.
337
338 Since an integrative gene regulatory network analysis of TF–target interactions positioned TGA1
339 and its homolog TG4 as the most influential TFs in the nitrate response[79,80], we decide to test if
340 they play a role in the response to low temperature in RHs and low/high levels of Nitrogen
341 (**Figure S8**). As expected *tga1 tga4* double mutant failed to respond to low temperature and low
342 nitrogen while TGA1 OE showed a constitutive growth response regardless the temperature and
343 nitrogen levels. This confirms that nitrate, NRT1.1 and its downstream signaling pathway
344 including the transcriptional responses controlled by TGA1-TG4 act an important pathway in RH
345 growth at low temperature.
346
347 **Discussion**
348
349 Growth and development of plants and animals are based on nutrient and hormonal signaling
350 that constitute as the main regulatory networks in eukaryotes. Unraveling the functions of the
351 regulatory hubs and their detailed molecular mechanisms are critical for deeper understanding of
352 these signaling pathways. In all cells, there is a central hub composed by the evolutionarily
353 conserved TOR protein kinase that integrates nutrient and energy levels coupled to stress
354 signaling networks to further modulate cell growth[81–84]. In addition, the cell surface receptor FER
355 acts as a versatile sensor of signals coming from the environment[51,85,86]. Specifically, our study
356 uncovers a new molecular mechanism by which plants use FER-ROP2-TOR signaling pathway to
357 control RH elongation under low nutrient conditions, specifically nitrate, induced by low
358 temperature stress (**Figure 7**).
359
360 In this work, we discovered that the cell surface FER receptor regulates TOR apical localization
361 and further downstream activation, both controlling S6K phosphorylation linked to RH growth.
362 Based on the results obtained and previous evidences, here we propose a model in which the
363 FER-ROP2-TOR axis might be able to regulate the RH growth under low temperature with
364 remarked attention to variable nitrate conditions (**Figure 7**). In agreement with this, it was
365 previously shown that ROP2 in response to auxin is an upstream effector of TOR activation[44] and
366 by inorganic and organic nitrogen inputs[43]. In addition, FER was shown to directly activate the

367 TOR/RAPTOR1B signaling pathway under low inorganic and organic nitrogen conditions[52] and is
368 an upstream regulator of the ROPGEF4-ROP2 signaling pathway that controls ROS-mediated RH
369 development[47,87]. In addition, ROP2 promotes TOR accumulation close to the cell periphery[44],
370 suggesting that plasma membrane-localized FER together with ROP2 function in regulating the
371 relocation of TOR, close to the RH tip. Interestingly, such a local, non-genomic regulatory circuit
372 may also explain the rapid, cell-autonomous growth regulation in RH cells observed under
373 asymmetric conditions in the dual-flow-RootChip[6]. All these findings are in line with our results
374 and support the idea of the existence of the FER-ROP2-TOR pathway being highly relevant for RH
375 growth in a changing nutritional environment. Interestingly, we recently showed that FER
376 regulates localized protein synthesis during polar RH cell growth[5,88], suggesting that FER-TOR may
377 also regulates polar protein synthesis in RHs. All the data together clearly highlight a key role of
378 the FER-ROP2-TOR pathway as a core complex in sensing nutrients (e.g. nitrates) to direct RH
379 growth.
380
381 Nitrogen is an essential nutrient for plants that when scarce limits plant growth. Although
382 inorganic nitrogen (e.g. nitrate) is a major source of nitrogen for plants in soil, organic forms of
383 nitrogen, like amino acids, can also be assimilated by plants from soil[89,90]. Changes in nitrate
384 concentrations in the media mimicked this response at low temperature and NRT1.1 mutants are
385 insensitive at RH growth level regardless the temperature or nitrate levels. We hypothesize that
386 low nitrate in the media might rapidly induce the levels of mature-active RALF1 (and possibly
387 other RALF peptides), which might then activate the FER-ROP2-TOR pathway and the
388 downstream fast cell elongation effect to search for further nutrients sources. This autocrine
389 mechanism dependent on RALF1-FER growth activation has been demonstrated for RH[88], but not
390 in a context that involves low temperature/low nitrate and TOR pathway. It is expected that low
391 nitrates levels will impact on amino acid homeostasis. In line with our results, branched-chain
392 amino acids have been shown to serve as upstream activators of TOR in plants[40]. TOR is also
393 involved in mediating amino acid-derived metabolic regulatory signals that influence respiratory
394 activity and plant metabolic rate[91]. Specifically, a total of 15 proteinogenic amino acids can
395 reactivate TOR under inorganic-N starvation conditions[43]. In addition, the FER-TOR pathway
396 responds to Gln, Asp, and Gly, reinforcing that amino acids serve as conserved upstream
397 regulators of the TOR signaling pathway in animals and plants[52]. It is tempting to speculate that
398 under low nitrates condition (and low temperature), the RH cell compensates with an altered
399 amino acid homeostasis to trigger TOR activation linked fast cell growth.
400
401 Finally, several questions in our proposed model remain to be answered in future studies. How
402 does low nitrate concentration (low temperature) triggers FER-TOR activation?. Does RALF1 and
403 other RALFs respond to low nitrate to activate FER?. Does FER activate NRT1.1 directly?. Recently,
404 it was shown that FER-regulated ROP2 triggers a new mechanism of negative regulation in the

405 case of rhizosphere microorganisms such as *Pseudomonas*[76]. Although not tested here, FER-
406 ROP2-TOR signaling coupled to enhanced RH growth under low temperature (low-nutrients)
407 might be linked to the root growth in specific soil conditions to select favorable microbiota in the
408 soil. This pathway may integrate complex signals from soil nutrients and microbiota in the
409 rhizosphere to plant root cell growth mechanism.

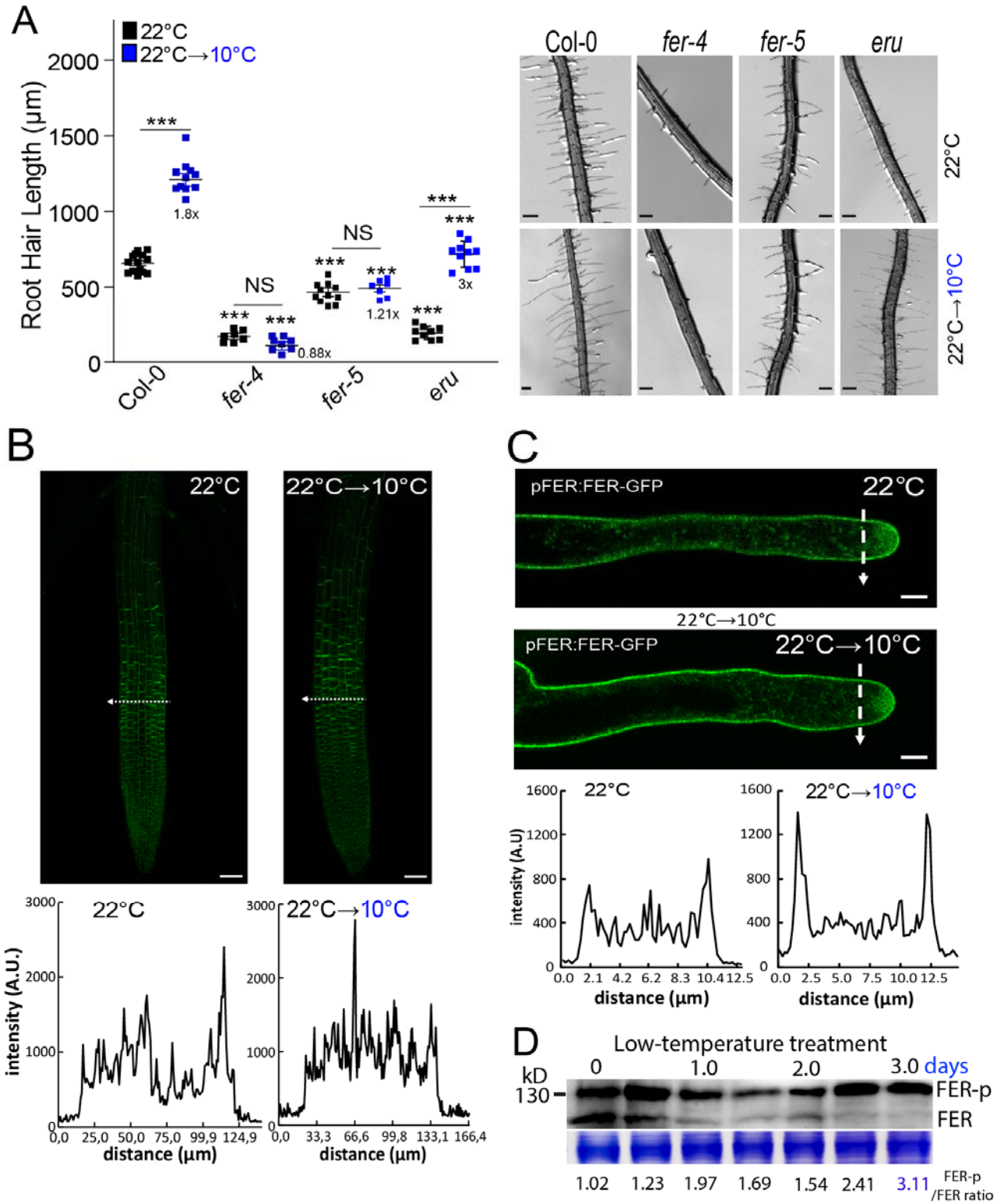


**Figure 1. High levels of FER in its phosphorylated form are required to trigger the low temperature RH growth.**

413 (**A**) Scatterplot of RH length of Col-0, of *fer-4*, *fer-5*, and *eru* mutants grown at 22°C or at 10°C. RH
414 growth is enhanced at low temperature in Wt Col-0 and *eru* mutant but not in the *fer-4* and *fer-5*
415 mutants. Each point is the mean of the length of the 10 longest RHs identified in the maturation
416 zone of a single root. Data are the mean ± SD (N=10 roots), two-way ANOVA followed by a
417 Tukey–Kramer test; (***) $p$ <0.001, NS= non-significant. Results are representative of three
418 independent experiments. Asterisks indicate significant differences between Col-0 and the
419 corresponding genotype at the same temperature or between the same genotype at different
420 temperatures. Representative images of each genotype are shown on the right. Scale bars= 300
421 µm. Numbers under the plots represents RH growth ratio 10°C/22°C.
422 (**B-C**) Increased level of FER in root cells after its activation by low temperature. (**B**) Confocal
423 images of root apex of a fluorescent translational reporter line of FER (*pFER:FER-GFP*) at 22°C and
424 after transfer from ambient to low temperature (22°C→10°C). On the Bottom: semi-quantitative
425 evaluation of the GFP fluorescence intensity across the root tip at 22°C and after transfer from
426 ambient to low temperature at the transition zone, indicated by a interrupted white line.
427 Fluorescence intensity is expressed in arbitrary units (AU), N=4-6 roots. Results are representative
428 of three independent experiments. Scale bars: 50 µm.
429 (**C**) Confocal images of short root hairs of a fluorescent translational reporter line of FER
430 (*p*FER:FER-GFP) at 22°C and after transfer from ambient to low temperature (22°C→10°C) On the
431 bottom: semi-quantitative evaluation of the GFP fluorescence intensity across the subapical root
432 hair zone at 22°C and after transfer from ambient to low temperature, indicated by a interrupted
433 white line. Fluorescence intensity is expressed in arbitrary units (A.U.), N=6-8 roots, 8-11 root
434 hairs. Results are representative of three independent experiments. Scale bars=5 µm.
435 (**D**) Phosphorylation levels on FER (FER-p in *p*FER:FER-GFP) increases after 3 days at low
436 temperature in roots. Protein loading control (Coomasie Blue) is indicated below. FER-p/FER
437 ratios were analyzed by ImageJ.

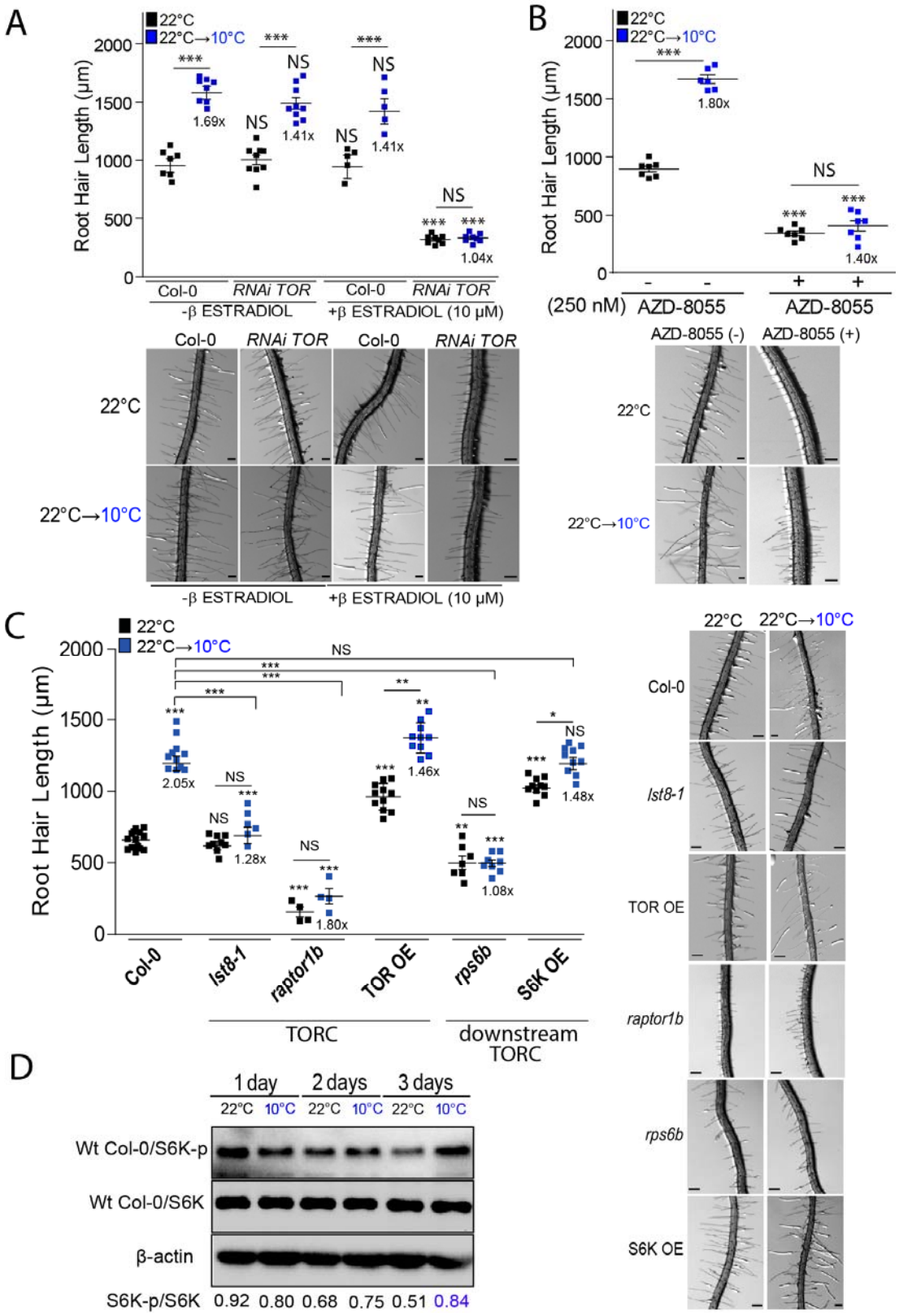


**Figure 2. TORC signaling pathway is required for low temperature triggered RH growth.**

441 (**A**) Scatterplot of RH length of Col-0 and *tor-es* line grown at 22°C or at 10°C. Differential growth
442 of RH at low temperature is suppressed in the estradiol inducible *RNAi TOR* line. Each point is the
443 mean of the length of the 10 longest RHs identified in the maturation zone of a single root. Data
444 are the mean ± SD (N=7-10 roots), two-way ANOVA followed by a Tukey–Kramer test; (***)
445 $p<0.001$, NS=non-significant. Results are representative of three independent experiments.
446 Asterisks indicate significant differences between Col-0 and the corresponding genotype at the
447 same temperature or between the same genotype at different temperatures. Representative
448 images of each line are shown below. Scale bars=300 µm. Numbers under the plots represents
449 RH growth ratio 10°C/22°C.
450 (**B**) Differential growth of RH at low temperature is abolished in the Col-0 treated with 250 nM of
451 TOR inhibitor, AZD-8055. Each point is the mean of the length of the 10 longest RHs identified in
452 the maturation zone of a single root. Data are the mean ± SD (N=7 roots), two-way ANOVA
453 followed by a Tukey–Kramer test; (***) $p<0.001$, NS=non-significant. Results are representative
454 of three independent experiments. Asterisks indicate significant differences between Col-0 and
455 the corresponding genotype at the same temperature or between the same genotype at different
456 temperatures. Representative images of each line are shown below. Scale bars=300 µm. Numbers
457 under the plots represents RH growth ratio 10°C/22°C.
458 (**C**) RH elongation of TOR and downstream TOR signaling pathway mutants under low
459 temperature. Each point is the mean of the length of the 10 longest RHs identified in the
460 maturation zone of a single root. Data are the mean ± SD (N=7-12 roots), two-way ANOVA
461 followed by a Tukey–Kramer test; (*) $p<0.05$, (**) $p<0.01$, (***) $p<0.001$, NS=non-significant.
462 Results are representative of three independent experiments. Asterisks indicate significant
463 differences between Col-0 and the corresponding genotype at the same temperature or between
464 the same genotype at different temperatures. Representative images of each line are shown on
465 the right. Scale bars=300 µm. Numbers under the plots represents RH growth ratio 10°C/22°C.
466 (**D**) Analysis of the phosphorylation state of S6K (S6K-p/S6K ratio) in Col-0. A representative
467 immunoblot is shown of two biological replicates (see **Supplementary Material 1**). S6K-p/S6K
468 ratio was analyzed by ImageJ.

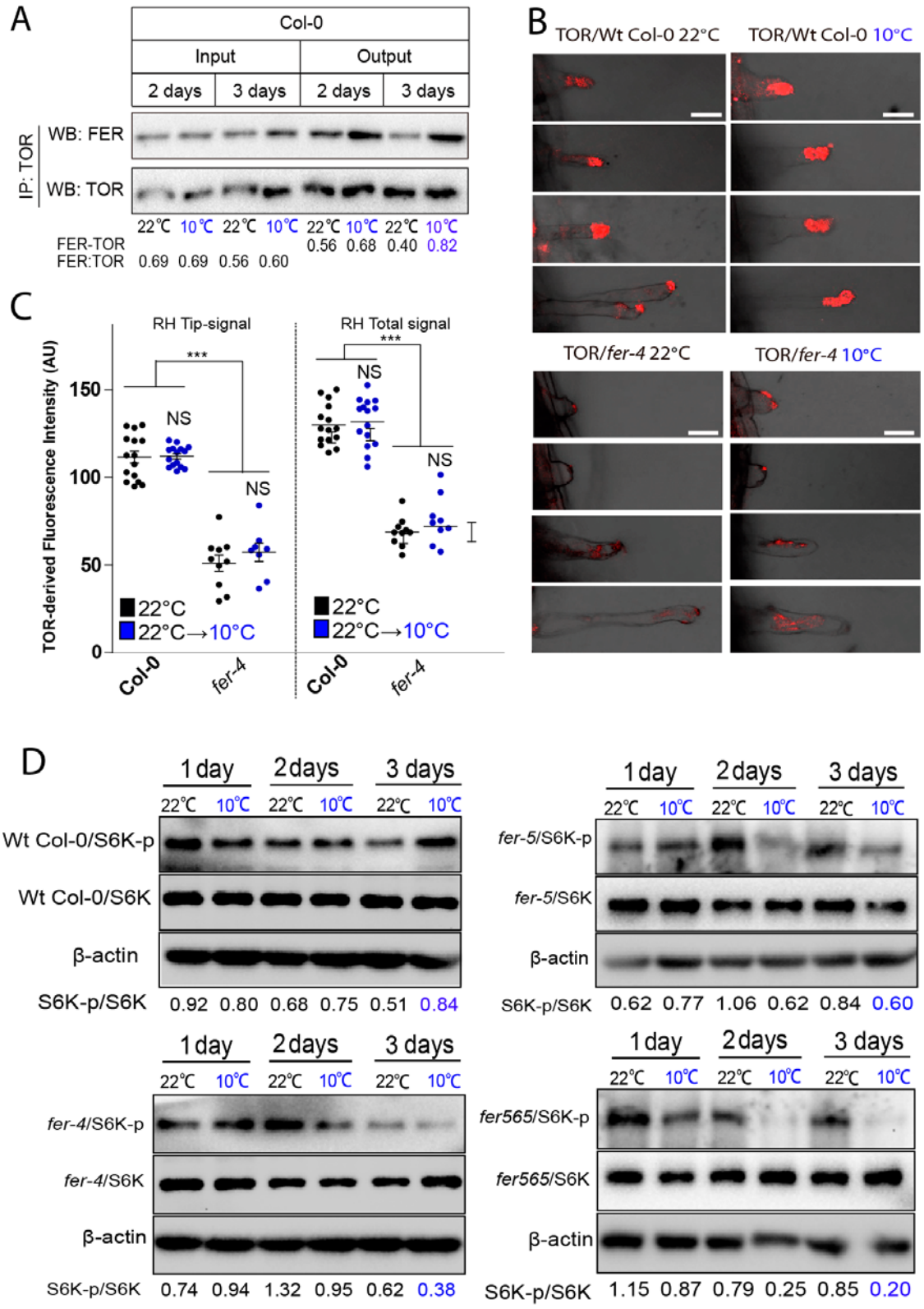


**Figure 3. FER controls polar TOR localization and subsequent activation thus increasing phosphorylation of S6K under low temperature.**

473 (**A**) Enhanced FER-TOR interaction at low temperature in roots by Immunoprecipitation (IP). A
474 representative experiment of three replicates is shown (see **Supplementary Material 1**).
475 (**B**) Representative images showing TOR immunolocalization in RHs is FER-dependent. Scale
476 bar=10 µm. Control images with the pre-immune serum as primary antibody are included in
477 **Figure S3**.
478 (**C**) Apical and total TOR signal quantification in RHs showed in (B). A ROI at the RH tip of the
479 fluorescent signal or at the entire RH TOR-derived fluorescent signal was measured. Fluorescence
480 AU data are the mean ± SD (N=10-15 root hairs), two-way ANOVA followed by a Tukey–Kramer
481 test; (***) $p<0.001$, NS= non-significant. Results are representative of two independent
482 experiments. Asterisks on the graph indicate significant differences between genotypes.
483 (**D**) Analysis of the phosphorylation state of S6K in Wt Col-0, *fer-4, fer-5*, and $FER^{K565R}$ mutants
484 Arabidopsis roots. Phosphorylation of S6K (S6K-p) is enhanced at low temperature and requires
485 FER active kinase. A representative immunoblot is shown of three biological replicates (see
486 **Supplementary Material 1**). S6K-p/S6K ratio was analyzed by Image J. Wt Col-0 immublot is the
487 same of the Figure 2D.

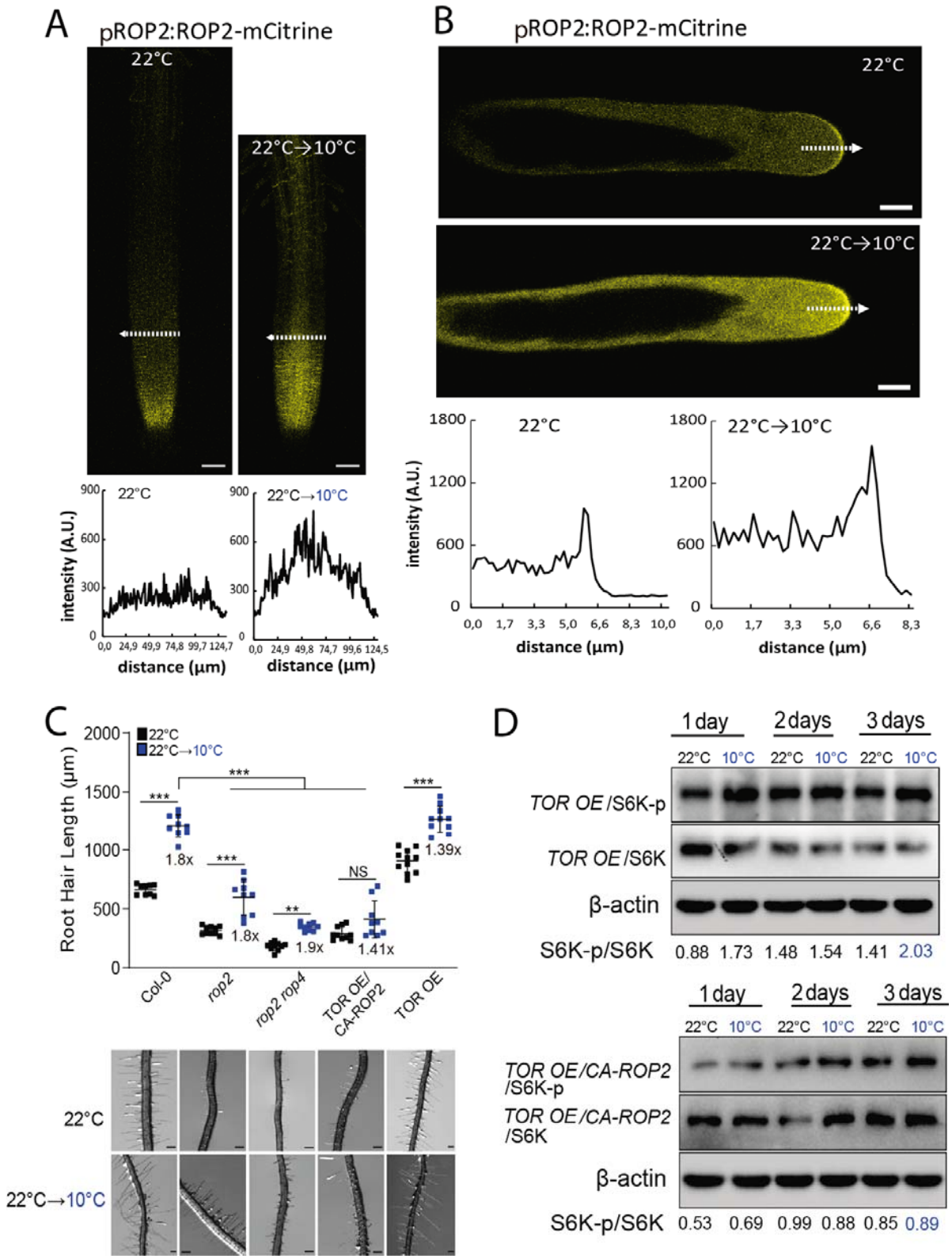


**Figure 4. ROP2 is required to triggers RH growth at low temperature.**

491 (**A-B**) Increased level of ROP2 after its activation by low temperature.
492 (**A**) Confocal images of root apex of a fluorescent translational reporter line of ROP2
493 (*p*ROP2:ROP2-mCitrine) at 22°C (A) and after transfer from ambient to low temperature (22°C→
494 10°C). On the bottom: semi-quantitative evaluation of the mCitrine fluorescence intensity across
495 the root tip at 22°C and after transfer from ambient to low temperature at the transition zone,
496 indicated by a interrupted white line. Fluorescence intensity is expressed in arbitrary units (A.U.),
497 N=4-5 roots. Results are representative of three independent experiments. Scale bars=50 µm.
498 (**B**) Increased level of ROP2 in the plasma membrane of RHs after its activation by low
499 temperature. Confocal images of short RHs of a fluorescent translational reporter line of ROP2
500 (ROP2p:ROP2-mCitrine) at 22°C and after transfer from ambient to low temperature (22°C→10°
501 C). On the bottom: semi-quantitative evaluation of the mCitrine fluorescence intensity across the
502 RH apex at 22°C and after transfer from ambient to low temperature, indicated by a interrupted
503 white line. Fluorescence intensity is expressed in arbitrary units (A.U.), N=4-5 roots, 6-8 root
504 hairs. Results are representative of three independent experiments. Scale bars=5 µm.
505 (**C**) ROP2 is required for RH at low temperature meanwhile *rop2, rop2 rop4* and *CA-ROP2/TOR OE*
506 blocks RH growth. Each point is the mean of the length of the 10 longest RHs identified in a single
507 root. Data are the mean ± SD (N=10-15 roots), two-way ANOVA followed by a Tukey–Kramer test;
508 (**) $p<0.01$, (***) $p<0.001$. Results are representative of three independent experiments.
509 Asterisks indicate significant differences. Representative images of each line are shown below.
510 Scale bars=300 µm. Numbers under the plots represents RH growth ratio 10°C/22°C.
511 (**D**) Analysis of the phosphorylation state of S6K in *TOR OE* and *TOR OE /CA-ROP2* Arabidopsis
512 roots. Phosphorylation of S6K (S6K-p) is enhanced in *TOR OE* and suppressed in *TOR OE*/ROP2-CA.
513 A representative immunoblot is shown of three biological replicates (see **Supplementary**
514 **Material 1**). S6K-p/S6K ratio was analyzed by Image J.

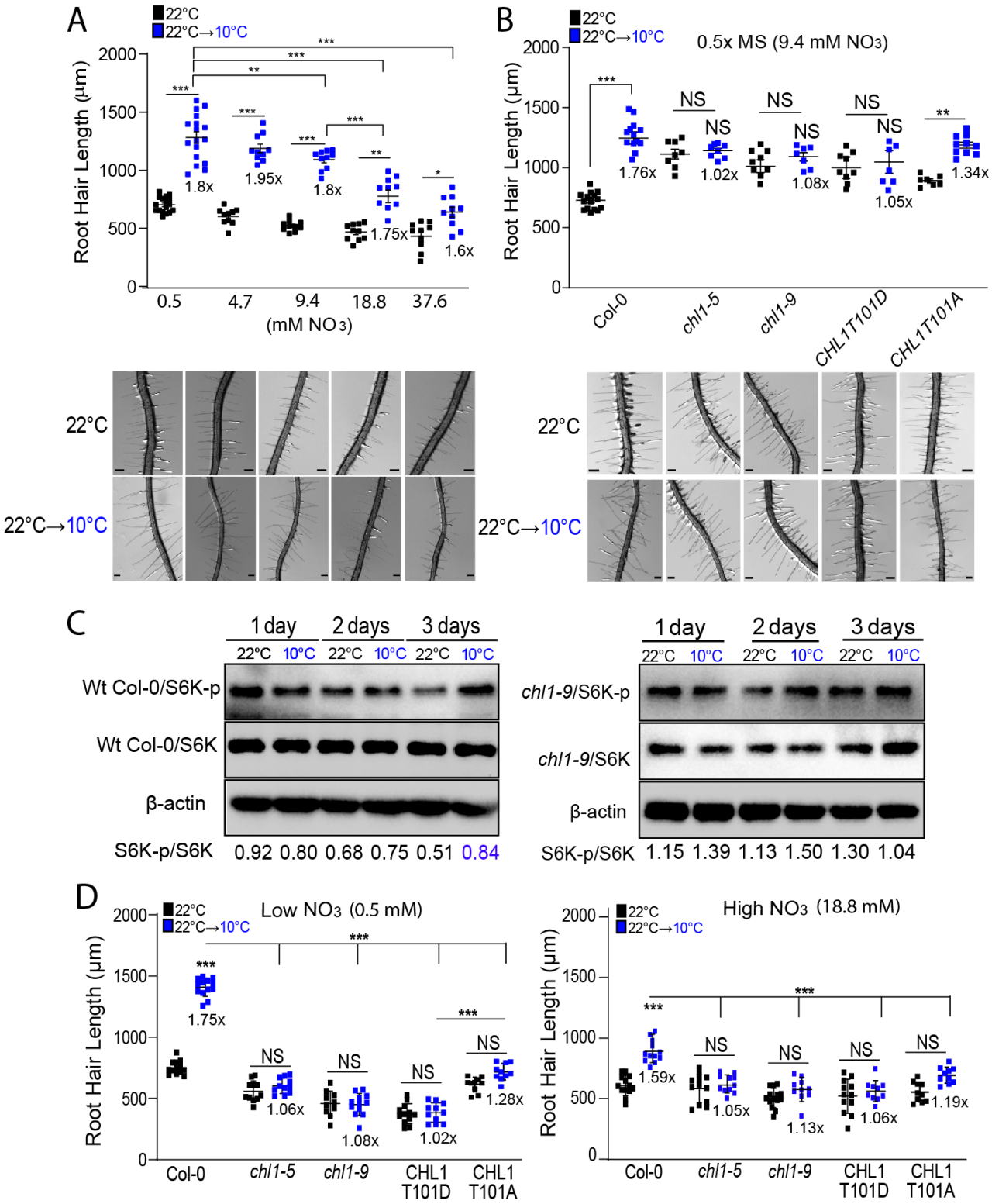


**Figure 5. Nitrate acts as a RH growth signal perceived by NRT1.1 and triggered by TOR pathway at low temperature growth.**

519 (**A**) High nitrate supplemented in M407 media (18.8 and 37.6 mM) partially suppresses low
520 temperature enhanced RH growth in Wt Col-0 plants. Each point is the mean of the length of the
521 10 longest RHs identified in the maturation zone of a single root. Data are the mean ± SD (N=10
522 roots), two-way ANOVA followed by a Tukey–Kramer test; (***) $p<0.001$. Results are
523 representative of three independent experiments. Asterisks indicate significant differences
524 between 0.5mM N concentration and every other N concentration at the same temperature or
525 between the same N concentrations at different temperatures. Representative images of Col-0
526 under the different nitrate concentrations are shown below. Scale bars=300 µm. Numbers under
527 the plots represents RH growth ratio 10°C/22°C.
528 (**B**) Low temperature RH growth is regulated by the nitrate sensor NRT1.1 (CHL1). Scatter-plot of
529 RH length of Col-0 and NRT1.1 mutants in 0.5X MS (contains 9.4 mM Nitrates) grown at 22°C or
530 10°C. Each point is the mean of the length of the 10 longest RHs identified in the maturation zone
531 of a single root. Data are the mean ± SD (N=10-15 roots), two-way ANOVA followed by a Tukey–
532 Kramer test; (***) $p<0.001$, NS=non-significant. Results are representative of three independent
533 experiments. Asterisks indicate significant differences between Col-0 and the corresponding
534 genotype at the same temperature or between the same genotype at different temperatures.
535 Representative images of each line are shown below. Scale bars=300 µm. Numbers under the
536 plots represents RH growth ratio 10°C/22°C.
537 (**C**) Analysis of the phosphorylation state of S6K in Wt Col-0 and *chl1-9* mutant roots. A
538 representative immunoblot is shown of three biological replicates (see **Supplementary Material**
539 **1**). S6K-p/S6K ratio was analyzed by ImageJ. Wt Col-0 immunoblot is the same of the Figure 2D
540 and Figure3D.
541 (**D**) RH growth responses under high and low nitrate (18.8 mM and 0.5 mM, respectively) in Wt
542 Col-0, *chl1-5*, *chl1-9* mutants, and $CHL1^{T101D}$ grown at 22°C or 10°C. Each point is the mean of the
543 length of the 10 longest RHs identified in the maturation zone of a single root. Data are the mean
544 ± SD (N=10-15 roots), two-way ANOVA followed by a Tukey–Kramer test; (***) $p<0.001$, NS= non-
545 significant. Results are representative of three independent experiments. Asterisks indicate
546 significant differences between Col-0 and the corresponding genotype at the same temperature
547 or between the same genotype at different temperatures. Numbers under the plots represents
548 RH growth ratio 10°C/22°C.

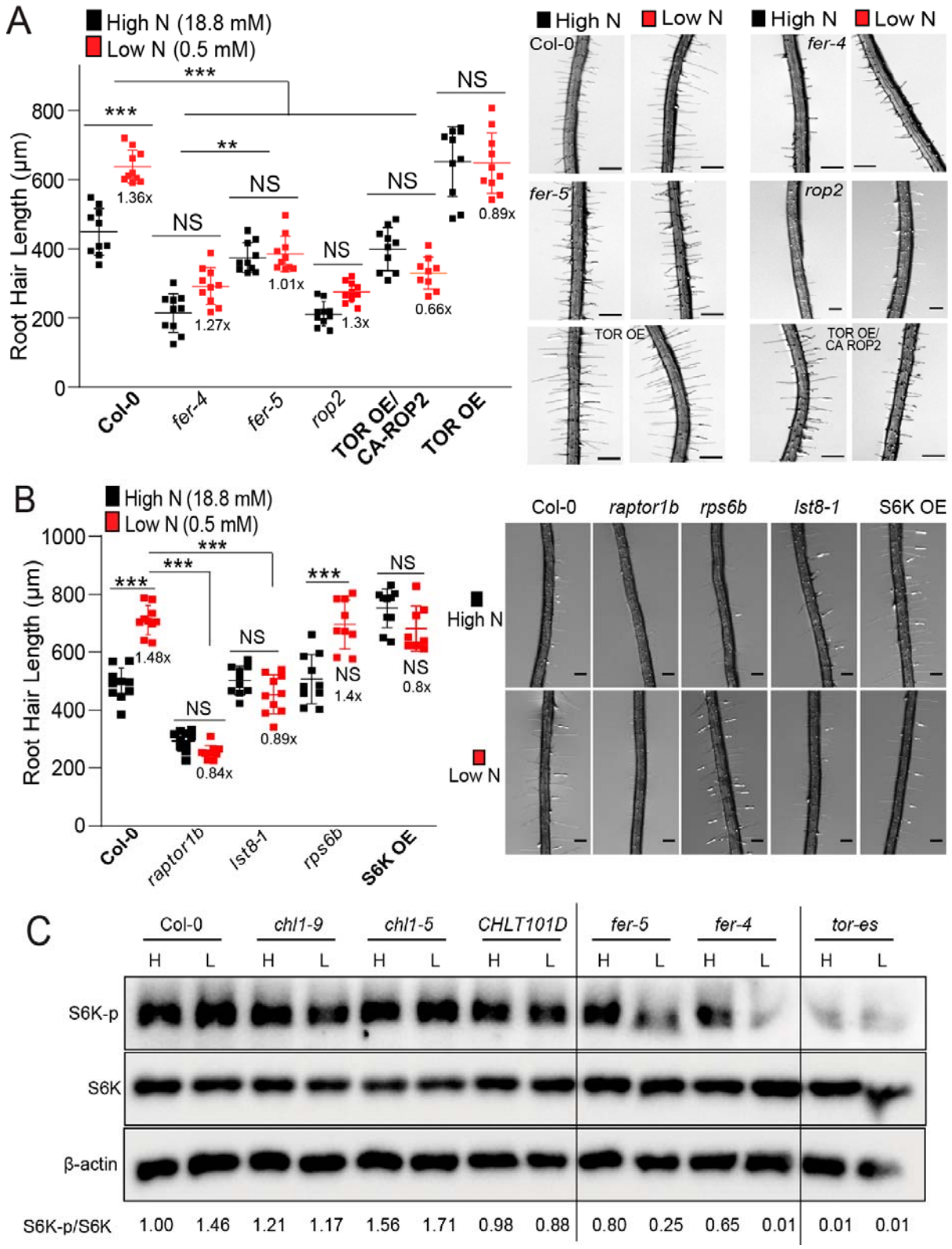


**Figure 6. Low nitrate perception relays in FER, ROP2 and TOR to trigger RH growth.**

552 (**A**) Scatterplot of RH length of Col-0, *fer-4*, *fer-5*, *rop2*, TOR OE/CA-ROP2 and TOR OE grown in
553 low (0.5 mM) and high nitrate (18.8 mM) conditions in M407 media, both at 22°C. Each point is
554 the mean of the length of the 10 longest RHs identified in the maturation zone of a single root.
555 Data are the mean ± SD (N=10 roots), two-way ANOVA followed by a Tukey–Kramer test; (**)
556 $p<0.01$, (***) $p<0.001$, NS=non-significant. Results are representative of three independent
557 experiments. Asterisks indicate significant differences between the same genotype at different N
558 concentration or between different genotypes at the same N concentration. Representative
559 images of each line are shown on the right. Scale bars=300 µm. Numbers under the plots
560 represents RH growth ratio low N/high N.
561 (**B**) Scatterplot of RH length of Col-0, *raptor1b*, *lst8-1*, *rps6b* and S6K OE mutants grown in low
562 and high N conditions. Each point is the mean of the length of the 10 longest RHs identified in the
563 maturation zone of a single root. Data are the mean ± SD (N=10 roots), two-way ANOVA followed
564 by a Tukey–Kramer test; (***) $p<0.001$, NS=non-significant. Results are representative of three
565 independent experiments. Asterisks indicate significant differences between the same genotype
566 at different N concentration or between different genotypes at the same N concentration.
567 Numbers under the plots represents RH growth ratio low N/high N.
568 (**C**) Analysis of the phosphorylation state of S6K in Wt Col-0, in NRT1.1 mutants (*chl1-9*, *chl1-5*,
569 CHLT101D), and in FER mutants (*fer-4*, *fer-5*, and $FER^{K565R}$). A representative immunoblot is shown
570 of a two biological replicates (see **Supplementary Material 1**). S6K-p/S6K ratio was analyzed by
571 Image J.

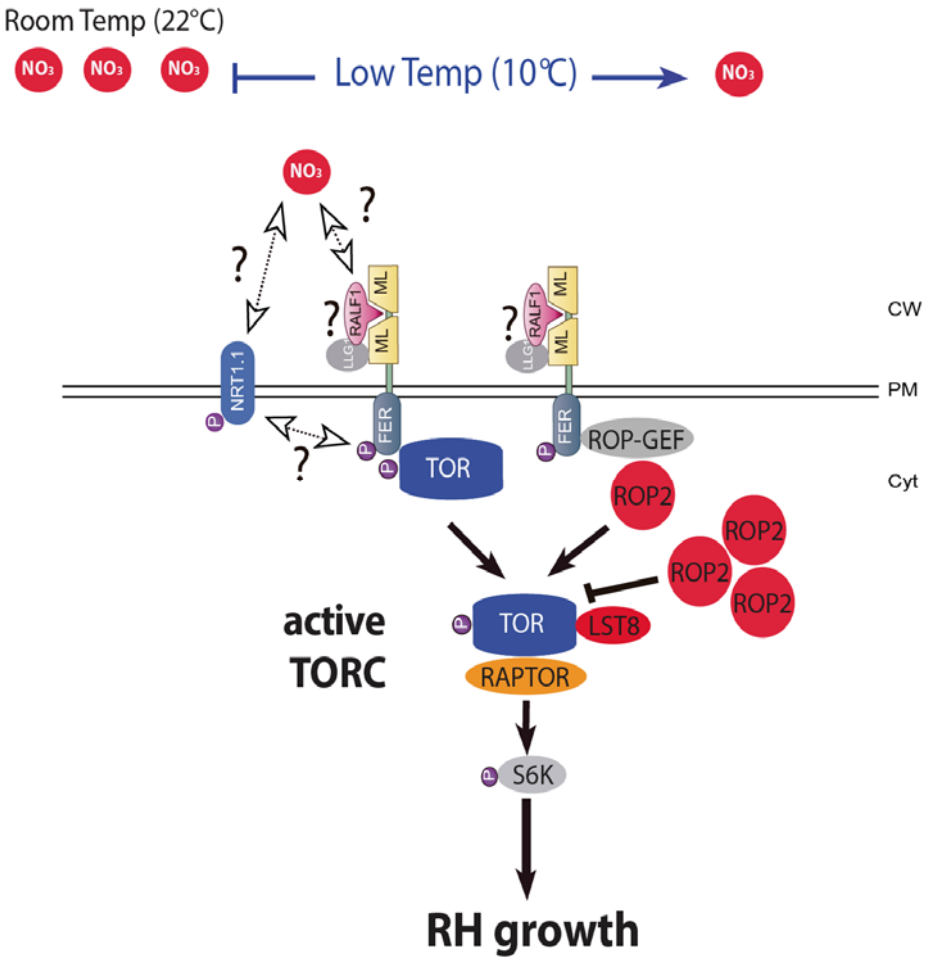


**Figure 7. Model of FER-ROP2-TOR function in RH elongation at limited nutrient availability caused by low temperature.** The model is based on the current evidence shown in this work and together with previous works. We have demonstrated that low temperature and nitrate conditions trigger RH elongation response through activation of the receptor kinase FERONIA. FERONIA triggers further activation of TOR either via direct binding to TOR (Left) or induction of the GTPase ROP2-TOR-S6K1 signaling axis via activation of GTPase ROP2 (Right). However, high levels of active ROP2 are able to negatively repress TORC activity. FERONIA can also activate NRT1.1 to promote RH elongation. Several questions (?) remain to be answered in future studies such as how low nitrate (triggered by low temperature) modulates FER-TOR activation? Does FER activate NRT1.1 directly? Do RALF1 and other RALFs respond to low nitrate to activate FER and downstream FER-TOR signaling?

585 **Experimental Procedures**

586

587 **Plant Material and Growth Conditions.** *A. thaliana* Col-0 ecotype was used as a wild-type plant.
588 To test the low and high nitrate response a 0.5X M407 medium without N, P nor K (M407,
589 PhytoTechnology Laboratories, https://www.phytotechlab.com/) supplemented with 0.8% plant
590 agar (Duchefa, Netherlands); 1.17mM MES, 0.625 mM $KH_2PO_4$ monobasic and 0.5mM $KNO_3$ (low
591 nitrate medium) 9.4mM, 18.8 mM and 37.6 mM $KNO_3$ (high nitrate medium) was used. Media
592 composition is detailed in **Table S1**. Plants were grown in the above media in continuous light
593 (120 µmol.seg$^{-1}$.m$^{-2}$) either: 8 days at 22°C in the case of *tor-es* line assay, 8 days at 22°C for
594 nitrate response assay or 5 days at 22°C + 3 days at 10°C for the low temperature and nitrate
595 response combination assay. For the rest of the low temperature experiments plants were grown
596 on regular 0.5X MS agar plates. For the imaging of fluorescence intensity distribution in root tips
597 and RH, seedlings were grown for 3 days at 22°C + 3-4 days at 10°C. All mutants and transgenic
598 lines are listed in **Table S2**. *chl1-5*, *chl1-9* and T101D mutants were kindly donated by Dr Yi-Fang
599 Tsay. *tor-es* was kindly donated by Dr Ezequiel Petrillo, *lst8-1*, *rps6b*, *raptor1b* and overexpressing
600 line S6K1 (S6K OE) kindly donated by Dr Elina Welchen and TOR OE and TOR OE/CA-ROP2 kindly
601 donated by Dr. Lyubov Ryabova.

602

603 **Pharmacological Treatments.** For all experiments, plants were grown first on solid 0.5X MS
604 medium at 22°C for 5 days in continuous light. According to the specific treatment plants were
605 transferred to plates containing regular solid 0.5X MS supplemented with 100nM IAA (auxin
606 treatment), 250 nM AZD-8055 (TOR inhibition) or 10 µM β-estradiol (*tor-es* line low temperature
607 treatment) and grown at 22°C for 5 days + 3 days at 10°C in continuous light. RH phenotype was
608 quantified after each 3 days span. For nitrate response treatment plants were transferred to
609 plates containing low or high nitrate solid media supplemented with 10 µM β-estradiol (*tor-es*
610 line), grown at 22°C for 3 days in continuous light and RH phenotype quantified.

611

612 **Root hair phenotype.** Seeds were surface sterilized and stratified in darkness for 3 days at 4°C.
613 Then grown *in vitro* on a specific condition and medium in a plant growth chamber in continuous
614 light (120 µmol.sec$^{-1}$.m$^{-2}$) at 22°C and/or 10°C. The quantitative analyses of RH phenotypes of Col-
615 0 and transgenic lines were made the last day of the growth conditions described in the two
616 previous sections. In the case of low temperature treatment, the measurements were done after
617 5 days at 22°C and after 3 days at 10°C. For that purpose, 10 fully elongated RH from the
618 maturation zone were measured per root under the same conditions from each treatment and
619 control. Images were captured using an Olympus SZX7 Zoom Stereo Microscope (Olympus, Japan)
620 equipped with a Q-Colors digital camera and Q Capture Pro 7 software (Olympus, Japan). Results
621 were expressed as the mean ± SD using the GraphPad Prism 8.0.1 (USA) statistical analysis

software. Results are representative of three independent experiments, each involving 7–20 roots.

**Confocal Microscopy.** For measurements of fluorescence intensity distributions after cold stress (22°C→10°C) in root tips and root hairs of *p*FER::FER-GFP and *p*ROP2::ROP2-mCitrine lines confocal laser scanning microscopy Zeiss LSM 710 (Carl Zeiss, Germany) was used. For image acquisition, 10x/0.3 NA EC Plan-Neofluar objective for root tips, and 40x/1.4 Oil DIC Plan-Apochromat objective for root hairs were used. GFP signal was excited with 488 nm argon laser at 4% laser power intensity and emission band of 493-549 nm. mCytrine signal was excited with 514 nm argon laser at 4% laser power intensity and emission band 519-583 nm. Fluorescence intensity measurements (in A.U.) were generated using Zen Black 2011 software (Carl Zeiss, Germany) and graphically edited in Microsoft Excel. Results are representative of three independent experiments, each involving 1–2 roots and 1 to 4 hairs per root.

**Co-IP assay**. For Co-IP assays using A/G agarose and an anti-TOR antibody[32], 30 µL of A/G beads (Thermo Fisher Scientific Inc., 20421) was resuspended and washed three times using NEB buffer (20 mM HEPES [pH 7.5], 40 mM KCl, 5 mM $MgCl_2$) before adding 8 µL of anti-TOR antibody or preimmune serum as a negative control[32] in a total volume of 500 µL of NEB buffer, followed by incubation for 4 h at 4 ˚C. Col-0 seedlings were first grown at 22 ˚C for 5 days then transferred to 22 ˚C or 10 ˚C for 2 days or 3 days. For protein extraction from plants, the collected materials were ground to a fine powder in liquid nitrogen and solubilized with NEB-T buffer (20 mM HEPES [pH 7.5], 40 mM KCl, 5 mM $MgCl_2$, 0.5% Triton X-100) containing 1 × protease inhibitor cocktail (Thermo Fisher Scientific Inc., 78430) and 1 × phosphatase inhibitor (Thermo Fisher Scientific Inc., 78420) and incubated for 1 h on the ice. The extracts were centrifuged at 16,000 g at 4 ˚C for 15 min, and the resultant supernatant was incubated with prepared antibody-beads from the above step. After overnight incubation at 4˚C with rotation, the agarose beads were washed five times with the NEB buffer and eluted with elution buffer (0.2 M glycine, 0.5% Triton X-100, pH 7.5). Anti-FER and anti-TOR antibodies[30] were used for immunoblotting to detect the immunoprecipitates.

**TOR immunolocalization**. Col-0 and *fer-4* seedlings were first grown at 22 ˚C for 5 days before transferred to 22 ˚C or 10 ˚C for 3 days. Then seedlings were collected and incubated for 10 min under vacuum (0.05 MPa) in phosphate-buffered saline (PBS) containing 4% paraformaldehyde and 0.1% Triton X-100. Seedlings were washed gently three times (10 min for each wash) in PBS and then the cell wall was digested in 2% Driselase (Sigma, D8037) in PBS for 18 min at 37 ˚C and washed five times with PBS. The permeability of the seedlings was increased by incubating them in 3% IGEPAL CA-630 (Sigma, 18896) and 10% DMSO in PBS for 18 min, followed by washed three

659 times with PBS. Seedlings were incubated in 2% bovine serum albumin (BSA) (Ameresco, 0332) in
660 PBS for 1.5 h and then incubated with primary TOR antibody[32] (antibody diluted 1:600 in 2% BSA)
661 for overnight at 4˚C. The seedlings were washed with PBS for five times. Fluorophore-labeled
662 secondary antibody (goat–mouse secondary antibody, diluted 1:600 in 2% BSA) was incubated
663 with the samples at 37˚C for 5 h in the dark. Seedlings were washed five times with PBS before
664 observation. Fluorescent signal detection and documentation were performed using a Nikon
665 confocal laser scanning microscope with a 560-nm band-pass filter for IF555 detection.
666
667 **S6K-p/S6K immunoblotting detection.** For immunological detection of S6K-p and S6K1/2, total
668 soluble proteins were extracted from 50 mg of plant materials grown as indicated previously with
669 100 µL 2 × Laemmli buffer supplemented with 1% Phosphatase Inhibitor Cocktail 2 (Thermo
670 Fisher Scientific Inc., 78430). Proteins were denatured for 10 min at 95˚C and separated on 10%
671 or 8% SDS-PAGE. Rabbit *At*TOR polyclonal antibodies (Abiocode, R2854-2), rabbit polyclonal
672 S6K1/2 antibodies (Agrisera, AS121855), and S6K1-p (phospho T449) antibody (Abcam,
673 ab207399) and ACTIN antibody (Abmart, M20009) were used for immunoblotting.
674
675 **Quantitative PCR (qPCR).** Total root RNA was extracted from plantlets grown *in vitro* at 22 ˚C and
676 10 ˚C using the RNeasy®Plant Mini Kit (QIAGEN, Germany). One microgram of total RNA was
677 reverse transcribed using an oligo$(dT)_{20}$ primer and the Super Script™ IV RT (Invitrogen,USA)
678 according to the manufacturer's instructions. cDNA was diluted 20-fold before PCR. *q*PCR was
679 performed on a LightCycler®480 Instrument II (Roche, USA) using 2 µL of 5X HOT
680 FIREPol®EvaGreen® qPCR Mix Plus(no ROX) (Solis BioDyne, Estonia), 2 µL of cDNA, and 0.25 µM of
681 each primer in a total volume of 10 µL per reaction. ACT2 (AT3G18780) gene was used as
682 reference for normalization of gene expression levels (ACT2 primers, F:
683 GGTAACATTGTGCTCAGTGGTGG R: CTCGGCCTTGGAGATCCACATC; TOR primers, F:
684 GAAGATGAAGATCCCGCTGA R: GCATCTCCAAGCATATTTACAGC[44]). The cycling conditions were: 95
685 °C for 12 min., 35 cycles of 95°C for 15 sec., 60°C for 1 min and finally a melting curve from 60°C
686 to 95 °C (0.05°/sec). Data were analyzed using the $\Delta\Delta C_t$ method[92] and LightCycler®480 Software,
687 version 1.5 (Roche). Two independent experiments with three biological and three technical
688 replicates per experiment, were performed.
689
690 **Qualitative determination of $KNO_3$ diffusion at 10°C and 22°C.** This method was adapted from a
691 previous protocol[93]. First, 25 ml of 0.8% agar-water media was prepared into plastic Petri dishes.
692 After gelation it was removed the center of the agar plate by using the rear part of a p1000 tip as
693 a puncher (removing a volume of approx. 200 µl of gel). After equilibration at either 10°C or 22°C
694 it was added 200 µl of liquid 0.8% Agar (at 40°C) containing 0,94M $KNO_3$ to fill up the well and
695 started the diffusion time. After 3 h of incubation, 20 µl agar disks were taken at different
696 distances from the border of the $KNO_3$ zone (from 5mm to 25mm in 5mm steps). For this

697 purpose, we used a Pasteur pipette as a puncher. The agar disks were incubated with 200 µl of
698 2mM diphenylamine ($(C_6H_5)2NH$) colorless solution in 14,4M $H_2SO_4$ with eventual shaking to
699 homogenize the reaction media. After 30 min we transferred 100ul of the bright blue resultant
700 reaction to a 96 well plate and measured OD at 595 nm. Serial dilutions showed deviations from
701 the expected linear behavior preventing the possibility of a robust quantitative assay. We used
702 high $KNO_3$ concentrations to prevent excessive dilution of the $NO_3^-$ below detection levels and
703 speed up the diffusion process.

**Acknowledgements**

We would like to thank Elina Welchen, Ezequiel Petrillo, Yi-Fang Tsay, Kriss Vissenberg for the seed lines. We thank NASC (Ohio State University) for providing T-DNA lines seed lines. J.M.E. is investigator of the National Research Council (CONICET) from Argentina. M.I. is supported by ANID FONDECYT POSTDOCTORADO [grant 3220138]. This work was supported by grants Natural Science Foundation of China (NSFC-32001974 and NSFC-31871396) to F.Y. and (NSFC-31900232) to L.S. and from ANPCyT (PICT2017-0066, and PICT2019-0015), by ANID – Programa Iniciativa Científica Milenio ICN17_022, NCN2021_010 and Fondo Nacional de Desarrollo Científico y Tecnológico [1200010] to J.M.E., by the Deutsche Forschungsgemeinschaft (DFG; GR4559_4-1, GR4559_5-1, EXC-2048/1 project ID 390686111) to G.G., and by the Czech Science Foundation GAČR (project Nr. 19-18675S) to J.Š.

**Author Contribution**

J.M.P performed most of the experiments, analysed the data and helped in the writing process of the manuscript. L.S. performed the S6K-p determinations, IP of TOR-FER and immunolocalization assay of TOR. L.K., M.O. and J.Š. provided live cell imaging data on FER and ROP2. V.B.G., J.M.P., T.U.I., M.A.I., M.M.R., S-Z., Y.S., R.A.G., M.S., L.A.R., J.M.A., G.G., J.S. helped in the data analysis and writing process of the manuscript. F.Y. designed research and analysed part of the data and J.M.E. designed research, analysed the data, supervised the project, and wrote the paper. All authors commented on the results and the manuscript. This manuscript has not been published and is not under consideration for publication elsewhere. All the authors have read the manuscript and have approved this submission.

**Competing financial interest**

The authors declare no competing financial interests. Correspondence and requests for materials should be addressed to F.Y. (feng_yu@hnu.edu.cn) and J.M.E. (Email: jestevez@leloir.org.ar).

732 **REFERENCES**

733


734 1. Šamaj, J., Müller, J., Beck, M., Böhm, N., and Menzel, D. (2006). Vesicular trafficking,
735 cytoskeleton and signalling in root hairs and pollen tubes. Trends Plant Sci. *11*, 594–600.
736 2. Pascale, A., Proietti, S., Pantelides, I.S., and Stringlis, I.A. (2019). Modulation of the Root
737 Microbiome by Plant Molecules: The Basis for Targeted Disease Suppression and Plant
738 Growth Promotion. Front. Plant Sci. *10*.
739 3. Vijayakumar, P., Datta, S., and Dolan, L. (2016). ROOT HAIR DEFECTIVE SIX-LIKE4 (RSL4)
740 promotes root hair elongation by transcriptionally regulating the expression of genes
741 required for cell growth. New Phytol. *212*, 944–953.
742 4. Kuběnová, L., Tichá, M., Šamaj, J., and Ovečka, M. (2022). ROOT HAIR DEFECTIVE 2
743 vesicular delivery to the apical plasma membrane domain during Arabidopsis root hair
744 development. Plant Physiol., kiab595.
745 5. Zhu, S., Estévez, J.M., Liao, H., Zhu, Y., Yang, T., Li, C., Wang, Y., Li, L., Liu, X., Pacheco, J.M.,
746 et al. (2020). The RALF1–FERONIA Complex Phosphorylates eIF4E1 to Promote Protein
747 Synthesis and Polar Root Hair Growth. Mol. Plant *13*, 698–716.
748 6. Stanley, C.E., Shrivastava, J., Brugman, R., Heinzelmann, E., van Swaay, D., and Grossmann,
749 G. (2018). Dual-flow-RootChip reveals local adaptations of roots towards environmental
750 asymmetry at the physiological and genetic levels. New Phytol. *217*, 1357–1369.
751 7. Yi, K., Menand, B., Bell, E., and Dolan, L. (2010). A basic helix-loop-helix transcription factor
752 controls cell growth and size in root hairs. Nat. Genet. *42*, 264–267.
753 8. Datta, S., Prescott, H., and Dolan, L. (2015). Intensity of a pulse of RSL4 transcription factor
754 synthesis determines Arabidopsis root hair cell size. Nat. Plants *1*, 1–6.
755 9. Moison, M., Pacheco, J.M., Lucero, L., Fonouni-Farde, C., Rodríguez-Melo, J., Mansilla, N.,
756 Christ, A., Bazin, J., Benhamed, M., Ibañez, F., et al. (2021). The lncRNA APOLO interacts
757 with the transcription factor WRKY42 to trigger root hair cell expansion in response to
758 cold. Mol. Plant *14*, 937–948.
759 10. Singha, S., Townsend, E.C. and Oberly, G.H. (1985). Mineral nutrient status of crabapple
760 and pear shoots cultured in vitro on varying commercial agars. J. Am. Soc. Hortic. Sci. *110*,
761 407-411.
762 11. Nonami, H., and Boyer, J.S. (1989). Turgor and Growth at Low Water Potentials. Plant
763 Physiol. *89*, 798–804.
764 12. Ghashghaie, J., Brenckmann, F., and Saugier, B. (1991). Effects of agar concentration on
765 water status and growth of rose plants cultured in vitro. Physiol. Plant. *82*, 73–78.
766 13. Buah, J.N., Kawamitsu, Y., Sato, S., and Murayama, S. (1999). Effects of Different Types and
767 Concentrations of Gelling Agents on the Physical and Chemical Properties of Media and the
768 Growth of Banana ( Musa spp.) in Vitro. Plant Prod. Sci. *2*, 138–145.
769 14. Pacheco, J.M., Mansilla, N., Moison, M., Lucero, L., Gabarain, V.B., Ariel, F., and Estevez,
770 J.M. (2021). The lncRNA APOLO and the transcription factor WRKY42 target common cell
771 wall EXTENSIN encoding genes to trigger root hair cell elongation. Plant Signal. Behav. *16*,
772 1920191.
773 15. Pacheco, J.M., Ranocha, P., Kasulin, L., Fusari, C.M., Servi, L., Aptekmann, A.A., Gabarain,
774 V.B., Peralta, J.M., Borassi, C., Marzol, E., et al. (2022). Apoplastic class III peroxidases

775 PRX62 and PRX69 promote Arabidopsis root hair growth at low temperature. Nat.
776 Commun. *13*, 1310.
777 16. Xiong, Y., and Sheen, J. (2014). The role of target of rapamycin signaling networks in plant
778 growth and metabolism. Plant Physiol. *164*, 499–512.
779 17. Dobrenel, T., Mancera-Martínez, E., Forzani, C., Azzopardi, M., Davanture, M., Moreau, M.,
780 Schepetilnikov, M., Chicher, J., Langella, O., Zivy, M., et al. (2016). The arabidopsis TOR
781 kinase specifically regulates the expression of nuclear genes coding for plastidic ribosomal
782 proteins and the phosphorylation of the cytosolic ribosomal protein S6. Front. Plant Sci. *7*,
783 1–16.
784 18. Saxton, R.A., and Sabatini, D.M. (2017). mTOR Signaling in Growth, Metabolism, and
785 Disease. Cell *168*, 960–976.
786 19. Tatebe, H., and Shiozaki, K. (2017). Evolutionary Conservation of the Components in the
787 TOR Signaling Pathways. Biomolecules *7*, 1–17.
788 20. Van Leene, J., Han, C., Gadeyne, A., Eeckhout, D., Matthijs, C., Cannoot, B., De Winne, N.,
789 Persiau, G., Van De Slijke, E., Van de Cotte, B., et al. (2019). Capturing the phosphorylation
790 and protein interaction landscape of the plant TOR kinase. Nat. Plants *5*, 316–327.
791 21. Menand, B., Desnos, T., Nussaume, L., Bergert, F., Bouchez, D., Meyer, C., and Robaglia, C.
792 (2002). Expression and disruption of the Arabidopsis TOR (target of rapamycin) gene. Proc.
793 Natl. Acad. Sci. U. S. A. *99*, 6422–6427.
794 22. Anderson, G.H., Veit, B., and Hanson, M.R. (2005). The Arabidopsis AtRaptor genes are
795 essential for post-embryonic plant growth. BMC Biol. *3*, 1–12.
796 23. Deprost, D., Truong, H.N., Robaglia, C., and Meyer, C. (2005). An Arabidopsis homolog of
797 RAPTOR/KOG1 is essential for early embryo development. Biochem. Biophys. Res.
798 Commun. *326*, 844–850.
799 24. Mahfouz, M.M., Kim, S., Delauney, A.J., and Verma, D.P.S. (2006). Arabidopsis TARGET of
800 RAPAMYCIN interacts with RAPTOR, which regulates the activity of S6 kinase in response to
801 osmotic stress signals. Plant Cell *18*, 477–490.
802 25. Yang, H., Rudge, D.G., Koos, J.D., Vaidialingam, B., Yang, H.J., and Pavletich, N.P. (2013).
803 MTOR kinase structure, mechanism and regulation. Nature *497*, 217–223.
804 26. Rexin, D., Meyer, C., Robaglia, C., and Veit, B. (2015). TOR signalling in plants. Biochem. J.
805 *470*, 1–14.
806 27. Salem, M.A., Li, Y., Wiszniewski, A., and Giavalisco, P. (2017). Regulatory-associated protein
807 of TOR (RAPTOR) alters the hormonal and metabolic composition of Arabidopsis seeds,
808 controlling seed morphology, viability and germination potential. Plant J. *92*, 525–545.
809 28. Moreau, M., Azzopardi, M., Clé ment, G., Dobrenel, T., Marchive, C., Renne, C., Martin-
810 Magniette, M.L., Taconnat, L., Renou, J.P., Robaglia, C., et al. (2012). Mutations in the
811 Arabidopsis homolog of LST8/GβL, a partner of the target of Rapamycin kinase, impair
812 plant growth, flowering, and metabolic adaptation to long days. Plant Cell *24*, 463–481.
813 29. McCready, K., Spencer, V., and Kim, M. (2020). The Importance of TOR Kinase in Plant
814 Development. Front. Plant Sci. *11*, 1–7.
815 30. Henriques, R., Magyar, Z., Monardes, A., Khan, S., Zalejski, C., Orellana, J., Szabados, L., De
816 La Torre, C., Koncz, C., and BÖgre, L. (2010). Arabidopsis S6 kinase mutants display
817 chromosome instability and altered RBR1-E2F pathway activity. EMBO J. *29*, 2979–2993.

818 31. Ahn, C.S., Han, J.A., Lee, H.S., Lee, S., and Pai, H.S. (2011). The PP2A regulatory subunit
819 Tap46, a component of the TOR signaling pathway, modulates growth and metabolism in
820 plants. Plant Cell *23*, 185–209.
821 32. Xiong, Y., and Sheen, J. (2012). Rapamycin and glucose-target of rapamycin (TOR) protein
822 signaling in plants. J. Biol. Chem. *287*, 2836–2842.
823 33. Patrick, R.M., Lee, J.C.H., Teetsel, J.R.J., Yang, S.H., Choy, G.S., and Browning, K.S. (2018).
824 Discovery and characterization of conserved binding of eIF4E 1 (CBE1), a eukaryotic
825 translation initiation factor 4E– binding plant protein. J. Biol. Chem. *293*, 17240–17247.
826 34. Xiong, Y., and Sheen, J. (2015). Novel links in the plant TOR kinase signaling network. Curr.
827 Opin. Plant Biol. *28*, 83–91.
828 35. Dobrenel, T., Caldana, C., Hanson, J., Robaglia, C., Vincentz, M., Veit, B., and Meyer, C.
829 (2016). TOR Signaling and Nutrient Sensing. Annu. Rev. Plant Biol. *67*, 261–285.
830 36. González, A., and Hall, M.N. (2017). Nutrient sensing and TOR signaling in yeast and
831 mammals . EMBO J. *36*, 397–408.
832 37. Bakshi, A., Moin, M., Madhav, M.S., and Kirti, P.B. (2019). Target of rapamycin, a master
833 regulator of multiple signalling pathways and a potential candidate gene for crop
834 improvement. Plant Biol. *21*, 190–205.
835 38. Pacheco, J.M., Canal, M.V., Pereyra, C.M., Welchen, E., Martínez-Noël, G.M.A., and
836 Estevez, J.M. (2021). The tip of the iceberg: emerging roles of TOR, and its regulatory
837 functions in plant cells. J. Exp. Bot. *72*, 4085–4101.
838 39. Dong, Y., Silbermann, M., Speiser, A., Forieri, I., Linster, E., Poschet, G., Allboje Samami, A.,
839 Wanatabe, M., Sticht, C., Teleman, A.A., et al. (2017). Sulfur availability regulates plant
840 growth via glucose-TOR signaling. Nat. Commun. *8*, 1–10.
841 40. Cao, P., Kim, S.J., Xing, A., Schenck, C.A., Liu, L., Jiang, N., Wang, J., Last, R.L., and Brandizzi,
842 F. (2019). Homeostasis of branched-chain amino acids is critical for the activity of TOR
843 signaling in Arabidopsis. Elife *8*, 1–24.
844 41. Schaufelberger, M., Galbier, F., Herger, A., de Brito Francisco, R., Roffler, S., Clement, G.,
845 Diet, A., Hörtensteiner, S., Wicker, T., and Ringli, C. (2019). Mutations in the Arabidopsis
846 ROL17/isopropylmalate synthase 1 locus alter amino acid content, modify the TOR
847 network, and suppress the root hair cell development mutant lrx1. J. Exp. Bot. *70*, 2313–
848 2323.
849 42. Sun, X., Chen, H., Wang, P., Chen, F., Yuan, L., and Mi, G. (2020). Low nitrogen induces root
850 elongation via auxin-induced acid growth and auxin-regulated target of rapamycin (TOR)
851 pathway in maize. J. Plant Physiol. *254*, 153281.
852 43. Liu, Y., Duan, X., Zhao, X., Ding, W., Wang, Y., and Xiong, Y. (2021). Diverse nitrogen signals
853 activate convergent ROP2-TOR signaling in Arabidopsis. Dev. Cell *56*, 1283-1295.e5.
854 44. Schepetilnikov, M., Makarian, J., Srour, O., Geldreich, A., Yang, Z., Chicher, J., Hammann, P.,
855 and Ryabova, L.A. (2017). GTP ase ROP 2 binds and promotes activation of target of
856 rapamycin, TOR , in response to auxin . EMBO J. *36*, 886–903.
857 45. Li, X., Cai, W., Liu, Y., Li, H., Fu, L., Liu, Z., Xu, L., Liu, H., Xu, T., and Xiong, Y. (2017).
858 Differential TOR activation and cell proliferation in Arabidopsis root and shoot apexes.
859 Proc. Natl. Acad. Sci. U. S. A. *114*, 2765–2770.
860 46. Carol, R.J., Takeda, S., Linstead, P., Durrant, M.C., Kakesova, H., Derbyshire, P., Drea, S.,

861 Zarsky, V., and Dolan, L. (2005). A RhoGDP dissociation inhibitor spatially regulates growth
862 in root hair cells. Nature *438*, 1013–1016.
863 47. Duan, Q., Kita, D., Li, C., Cheung, A.Y., and Wu, H.M. (2010). FERONIA receptor-like kinase
864 regulates RHO GTPase signaling of root hair development. Proc. Natl. Acad. Sci. U. S. A.
865 *107*, 17821–17826.
866 48. Kang, E., Zheng, M., Zhang, Y., Yuan, M., Yalovsky, S., Zhu, L., and Fu, Y. (2017). The
867 microtubule-associated protein MAP18 affects ROP2 GTPase activity during root hair
868 growth. Plant Physiol. *174*, 202–222.
869 49. Denninger, P., Reichelt, A., Schmidt, V.A.F., Mehlhorn, D.G., Asseck, L.Y., Stanley, C.E.,
870 Keinath, N.F., Evers, J.F., Grefen, C., and Grossmann, G. (2019). Distinct RopGEFs
871 Successively Drive Polarization and Outgrowth of Root Hairs. Curr. Biol. *29*, 1854-1865.e5.
872 50. Huang, G.Q., Li, E., Ge, F.R., Li, S., Wang, Q., Zhang, C.Q., and Zhang, Y. (2013). Arabidopsis
873 RopGEF4 and RopGEF10 are important for FERONIA-mediated developmental but not
874 environmental regulation of root hair growth. New Phytol. *200*, 1089–1101.
875 51. Xu, G., Chen, W., Song, L., Chen, Q., Zhang, H., Liao, H., Zhao, G., Lin, F., Zhou, H., and Yu, F.
876 (2019). FERONIA phosphorylates E3 ubiquitin ligase ATL6 to modulate the stability of 14-3-
877 3 proteins in response to the carbon/nitrogen ratio. J. Exp. Bot. *70*, 6375–6388.
878 52. Song, L., Xu, G., Li, T., Zhou, H., Lin, Q., Chen, J., Wang, L., Wu, D., Li, X., Wang, L., et al.
879 (2022). The RALF1-FERONIA Complex Interacts with and Activates TOR Signaling in
880 Response to Low Nutrients. Mol. Plant *0*.
881 53. Kwon, T., Alan Sparks, J., Liao, F., and Blancaflor, E.B. (2018). Erulus is a plasma membrane-
882 localized receptor-like kinase that specifies root hair growth by maintaining tip-focused
883 cytoplasmic calcium oscillations[OPEN]. Plant Cell *30*, 1173–1177.
884 54. Schoenaers, S., Balcerowicz, D., Breen, G., Hill, K., Zdanio, M., Mouille, G., Holman, T.J., Oh,
885 J., Wilson, M.H., Nikonorova, N., et al. (2018). The Auxin-Regulated CrRLK1L Kinase ERULUS
886 Controls Cell Wall Composition during Root Hair Tip Growth. Curr. Biol. *28*, 722-732.e6.
887 55. Xiong, Y., McCormack, M., Li, L., Hall, Q., Xiang, C., and Sheen, J. (2013). Glucose-TOR
888 signalling reprograms the transcriptome and activates meristems. Nature *496*, 181–186.
889 56. Montané, M.H., and Menand, B. (2013). ATP-competitive mTOR kinase inhibitors delay
890 plant growth by triggering early differentiation of meristematic cells but no developmental
891 patterning change. J. Exp. Bot. *64*, 4361–4374.
892 57. Escobar-Restrepo, J.M., Huck, N., Kessler, S., Gagliardini, V., Gheyselinck, J., Yang, W.C.,
893 and Grossniklaus, U. (2007). The Feronia receptor-like kinase mediates male-female
894 interactions during pollen tube reception. Science (80-. ). *317*, 656–660.
895 58. Haruta, M., Sabat, G., Stecker, K., Minkoff, B.B., and Sussman, M.R. (2014). A peptide
896 hormone and its receptor protein kinase regulate plant cell expansion. Science (80-. ). *343*,
897 408–411.
898 59. Chakravorty, D., Yu, Y., and Assmann, S.M. (2018). A kinase-dead version of FERONIA
899 receptor-like kinase has dose-dependent impacts on rosette morphology and RALF1-
900 mediated stomatal movements. FEBS Lett. *592*, 3429–3437.
901 60. Jones, M.A., Shen, J.J., Fu, Y., Li, H., Yang, Z., and Grierson, C.S. (2002). The arabidopsis
902 Rop2 GTPase is a positive regulator of both root hair initiation and tip growth. Plant Cell
903 *14*, 763–776.

904 61. Gendre, D., Baral, A., Dang, X., Esnay, N., Boutte, Y., Stanislas, T., Vain, T., Claverol, S.,
905 Gustavsson, A., Lin, D., et al. (2019). Rho-of-plant activated root hair formation requires
906 arabidopsis YIP4a/b gene function. Dev. *146*.
907 62. Vatter, T., Neuhäuser, B., Stetter, M., and Ludewig, U. (2015). Regulation of length and
908 density of Arabidopsis root hairs by ammonium and nitrate. J. Plant Res. *128*, 839–848.
909 63. Canales, J., Contreras-López, O., Álvarez, J.M., and Gutiérrez, R.A. (2017). Nitrate induction
910 of root hair density is mediated by TGA1/TGA4 and CPC transcription factors in Arabidopsis
911 thaliana. Plant J. *92*, 305–316.
912 64. Liu, B., Wu, J., Yang, S., Schiefelbein, J., and Gan, Y. (2020). Nitrate regulation of lateral root
913 and root hair development in plants. J. Exp. Bot. *71*, 4405–4414.
914 65. Ho, C.H., Lin, S.H., Hu, H.C., and Tsay, Y.F. (2009). CHL1 Functions as a Nitrate Sensor in
915 Plants. Cell *138*, 1184–1194.
916 66. Gojon, A., Krouk, G., Perrine-Walker, F., and Laugier, E. (2011). Nitrate transceptor(s) in
917 plants. J. Exp. Bot. *62*, 2299–2308.
918 67. Bouguyon, E., Brun, F., Meynard, D., Kubeš, M., Pervent, M., Leran, S., Lacombe, B., Krouk,
919 G., Guiderdoni, E., Zazímalová, E., et al. (2015). Multiple mechanisms of nitrate sensing by
920 Arabidopsis nitrate transceptor NRT1.1. Nat. Plants *1*, 15015.
921 68. Krouk, G., Lacombe, B., Bielach, A., Perrine-Walker, F., Malinska, K., Mounier, E., Hoyerova,
922 K., Tillard, P., Leon, S., Ljung, K., et al. (2010). Nitrate-regulated auxin transport by NRT1.1
923 defines a mechanism for nutrient sensing in plants. Dev. Cell *18*, 927–937.
924 69. Liu, K.-H., and Tsay, Y.-F. (2003). Switching between the two action modes of the dual-
925 affinity nitrate transporter CHL1 by phosphorylation. EMBO J. *22*, 1005–13.
926 70. Forde, B.G., and Walch-Liu, P. (2009). Nitrate and glutamate as environmental cues for
927 behavioural responses in plant roots. Plant, Cell Environ. *32*, 682–693.
928 71. Léran, S., Varala, K., Boyer, J.C., Chiurazzi, M., Crawford, N., Daniel-Vedele, F., David, L.,
929 Dickstein, R., Fernandez, E., Forde, B., et al. (2014). A unified nomenclature of nitrate
930 transporter 1/peptide transporter family members in plants. Trends Plant Sci. *19*, 5–9.
931 72. Wang, W., Hu, B., Li, A., and Chu, C. (2020). NRT1.1s in plants: Functions beyond nitrate
932 transport. J. Exp. Bot. *71*, 4373–4379.
933 73. Deprost, D., Yao, L., Sormani, R., Moreau, M., Leterreux, G., Bedu, M., Robaglia, C., and
934 Meyer, C. (2007). The Arabidopsis TOR kinase links plant growth, yield, stress resistance
935 and mRNA translation. EMBO Rep. *8*, 864–870.
936 74. ROBINSON, D., and RORISON, I.H. (1987). ROOT HAIRS AND PLANT GROWTH ATLOW
937 NITROGEN AVAILABILITIES. New Phytol. *107*, 681–693.
938 75. Deak, K.I., and Malamy, J. (2005). Osmotic regulation of root system architecture. Plant J.
939 *43*, 17–28.
940 76. Song, Y., Wilson, A.J., Zhang, X.C., Thoms, D., Sohrabi, R., Song, S., Geissmann, Q., Liu, Y.,
941 Walgren, L., He, S.Y., et al. (2021). FERONIA restricts Pseudomonas in the rhizosphere
942 microbiome via regulation of reactive oxygen species. Nat. Plants *7*, 644–654.
943 77. Bloch, D., Monshausen, G., Gilroy, S., and Yalovsky, S. (2011). Co-regulation of root hair tip
944 growth by ROP GTPases and nitrogen source modulated pH fluctuations. Plant Signal.
945 Behav. *6*, 426–429.
946 78. Salem, M.A., Li, Y., Bajdzienko, K., Fisahn, J., Watanabe, M., Hoefgen, R., Schöttler, M.A.,

947 and Giavalisco, P. (2018). RAPTOR controls developmental growth transitions by altering
948 the hormonal and metabolic balance. Plant Physiol. *177*, 565–593.
949 79. Vidal, E.A., Alvarez, J.M., Araus, V., Riveras, E., Brooks, M.D., Krouk, G., Ruffel, S., Lejay, L.,
950 Crawford, N.M., Coruzzi, G.M., et al. (2020). Nitrate in 2020: Thirty years from transport to
951 signaling networks. Plant Cell *32*, 2094–2119.
952 80. Alvarez, J.M., Riveras, E., Vidal, E.A., Gras, D.E., Contreras-López, O., Tamayo, K.P.,
953 Aceituno, F., Gómez, I., Ruffel, S., Lejay, L., et al. (2014). Systems approach identifies TGA1
954 and TGA4 transcription factors as important regulatory components of the nitrate
955 response of Arabidopsis thaliana roots. Plant J. *80*, 1–13.
956 81. Wullschleger, S., Loewith, R., and Hall, M.N. (2006). TOR signaling in growth and
957 metabolism. Cell *124*, 471–484.
958 82. Wang, P., Zhao, Y., Li, Z., Hsu, C.C., Liu, X., Fu, L., Hou, Y.J., Du, Y., Xie, S., Zhang, C., et al.
959 (2018). Reciprocal Regulation of the TOR Kinase and ABA Receptor Balances Plant Growth
960 and Stress Response. Mol. Cell *69*, 100-112.e6.
961 83. Wu, Y., Shi, L., Li, L., Fu, L., Liu, Y., Xiong, Y., and Sheen, J. (2019). Integration of nutrient,
962 energy, light, and hormone signalling via TOR in plants. J. Exp. Bot. *70*, 2227–2238.
963 84. Fu, L., Wang, P., and Xiong, Y. (2020). Target of Rapamycin Signaling in Plant Stress
964 Responses. Plant Physiol. *182*, 1613–1623.
965 85. Yang, T., Wang, L., Li, C., Liu, Y., Zhu, S., Qi, Y., Liu, X., Lin, Q., Luan, S., and Yu, F. (2015).
966 Receptor protein kinase FERONIA controls leaf starch accumulation by interacting with
967 glyceraldehyde-3-phosphate dehydrogenase. Biochem. Biophys. Res. Commun. *465*, 77–
968 82.
969 86. Yeats, T.H., Sorek, H., Wemmer, D.E., and Somerville, C.R. (2016). Cellulose Deficiency Is
970 Enhanced on Hyper Accumulation of Sucrose by a H+-Coupled Sucrose Symporter. Plant
971 Physiol. *171*, 110–124.
972 87. Yu, F., Qian, L., Nibau, C., Duan, Q., Kita, D., Levasseur, K., Li, X., Lu, C., Li, H., Hou, C., et al.
973 (2012). FERONIA receptor kinase pathway suppresses abscisic acid signaling in Arabidopsis
974 by activating ABI2 phosphatase. Proc. Natl. Acad. Sci. U. S. A. *109*, 14693–14698.
975 88. Zhu, S., Martínez Pacheco, J., Estevez, J.M., and Yu, F. (2020). Autocrine regulation of root
976 hair size by the RALF-FERONIA-RSL4 signaling pathway. New Phytol. *227*, 45–49.
977 89. Jones, D.L., Healey, J.R., Willett, V.B., Farrar, J.F., and Hodge, A. (2005). Dissolved organic
978 nitrogen uptake by plants—an important N uptake pathway? Soil Biol. Biochem. *37*, 413–
979 423.
980 90. Forsum, O., Svennerstam, H., Ganeteg, U., and Näsholm, T. (2008). Capacities and
981 constraints of amino acid utilization in Arabidopsis. New Phytol. *179*, 1058–1069.
982 91. O'Leary, B.M., Khim Oh, G.G., Lee, C.P., and Harvey Millar, A. (2020). Metabolite regulatory
983 interactions control plant respiratory metabolism via target of rapamycin (TOR) kinase
984 activation. Plant Cell *32*, 666–682.
985 92. Livak, K.J., and Schmittgen, T.D. (2001). Analysis of relative gene expression data using real-
986 time quantitative PCR and the 2-ΔΔCT method. Methods *25*, 402–408.
987 93. Grebber, K., and Karabinos, J.V. (1952). A study of the diphenylamine test for aliphatic
988 nitrocompounds. Journal of Research of the National Bureau of Standards *49*, 163-166.